



**Nebraska
Transportation
Center**



**MID-AMERICA
TRANSPORTATION CENTER**



Report SPR-P1 (08) P307

Final Report
26-1118-0085-001

Use of Ground Penetrating Radar for Construction Quality Assurance of Concrete Pavement

George Morcoux, Ph.D., P.E.

Associate Professor

The Charles W. Durham School of Architectural Engineering and Construction
University of Nebraska-Lincoln

Ece Erdogmus, Ph.D.

Associate Professor

2009

Nebraska Transportation Center
262 WHIT
2200 Vine Street
Lincoln, NE 68583-0851
(402) 472-1975

"This report was funded in part through grant[s] from the Federal Highway Administration [and Federal Transit Administration], U.S. Department of Transportation. The views and opinions of the authors [or agency] expressed herein do not necessarily state or reflect those of the U. S. Department of Transportation."

**Use of Ground Penetrating Radar for Construction
Quality Assurance of Concrete Pavement**

George Morcoux, Ph.D., P.E.
Associate Professor
Architectural Engineering & Construction
University of Nebraska-Lincoln

Ece Erdogmus, Ph.D.
Associate Professor
Architectural Engineering
University of Nebraska-Lincoln

A Report on Research Sponsored by

Nebraska Department of Roads

November 2009

Technical Report Documentation Page

1. Report No SPR-P1(08) P307	2. Government Accession No.	3. Recipient's Catalog No.	
4. Title and Subtitle Use of Ground Penetrating Radar for Construction Quality Assurance of Concrete Pavement		5. Report Date November 2009	
		6. Performing Organization Code	
7. Author/s George Morcoux and Ece Erdogmus		8. Performing Organization Report No. 26-1118-0085-0001	
9. Performing Organization Name and Address University of Nebraska-Lincoln 1110 South 67th St. Omaha, NE 68182-0178		10. Work Unit No. (TRAIS)	
		11. Contract or Grant No.	
12. Sponsoring Organization Name and Address Nebraska Department of Roads (NDOR) 1400 Highway 2 PO Box 94759 Lincoln, NE 68509		13. Type of Report and Period Covered Final Report	
		14. Sponsoring Agency Code MATC TRB RiP #13604	
15. Supplementary Notes			
16. Abstract Extracting concrete cores is the most common method for measuring the thickness of concrete pavement for construction quality control. Although this method provides a relatively accurate thickness measurement, it is destructive, labor intensive, and time consuming. Moreover, concrete cores are usually taken approximately every 750 ft, which may be inadequate for estimating the actual thickness profile of a pavement section; however extracting more cores would damage the pavement extensively and increase the labor cost and time excessively. Ground Penetrating Radar (GPR) is a well-established technique for subsurface exploration. Recently, GPR has been used for several transportation applications, such as measuring layer thickness in asphalt pavement, locating reinforcing bars and tendons, and detecting deteriorations and anomalies in concrete structures. The main advantages of GPR are speed, accuracy, and cost-effectiveness when scans are conducted on large areas. The objective of this project is to investigate the accuracy and cost-effectiveness of using GPR for measuring the thickness of concrete pavement for quality assurance purposes. The GPR systems GSSI SIR20 and SIR3000 with a high resolution 1.6 MHz ground coupled antenna were used in measuring the thickness of concrete pavement up to 14 in. thick. Several laboratory and field tests were carried out to determine the accuracy of the GPR measurement at different concrete ages and when various metal artifacts are used underneath the concrete to improve the reflectivity of the bottom surface. Testing results indicated that GPR is a cost-effective non-destructive technique for measuring the thickness of concrete pavement, compared to extracting concrete cores, and an accuracy of 1/8 in. can be achieved when appropriate reflectors and calibration cores are used.			
17. Key Words Keywords: GPR, Concrete Pavement Thickness.	18. Distribution Statement		
19. Security Classification (of this report) Unclassified	20. Security Classification (of this page) Unclassified	21. No. of Pages 72	22. Price

Form DOT F 1700.7 (8-72) Reproduction of form and completed page is authorized

Table of Contents

1 Introduction	1
1.1 Background	1
1.2 Objectives	2
2 Literature Review	4
2.1 GPR Methodology	4
2.2 Use of GPR for Pavement Layer Thickness Measurements	8
3 Laboratory Tests	13
3.1 Lab Test #1	13
3.2 Lab Test #2	18
4 Field Tests	32
4.1 Field Test #1	32
4.2 Field Test #2	36
4.2.2 Scan # 2	39
4.3 Field Test #3	42
4.4 Field Test #4	47
4.5 Field Test #5	51
5 Benefit-Cost Analysis	57
6 Summary and Conclusions	59
7 Implementation Plan	62
References	63
Appendix A	64

List of Figures

Figure 1.1 Core Measuring.....	2
Figure 2.1 GPR Principles.....	5
Figure 2.2 GPR survey of concrete pavement (Maierhofer 2003).....	9
Figure 2.3 Reinforced Concrete Slabs Used for GPR Testing at PKI labs by authors.....	12
Figure 3.1 Metal ring placed underneath a 12 in. thick concrete slab.....	13
Figure 3.2 GPR grid scan of the 12 in. thick concrete slab.....	14
Figure 3.3 Projection views of the tested slab.....	14
Figure 3.4 GPR single reflections at the reinforcing bars and metal ring.....	15
Figure 3.5 GPR single reflections at the reinforcing bars, metal ring, and metal strip.....	16
Figure 3.6 Form ties used in the lab test # 1.....	17
Figure 3.7 GPR signal reflections at the reinforcing bars and form tie.....	18
Figure 3.8 Location of the driveway built for lab test # 2.....	19
Figure 3.9 The five metal objects used in lab test # 2.....	19
Figure 3.10 Location of the five metal objects used in lab test # 2.....	21
Figure 3.11 Radargram of the scan performed on 12/21/2007.....	23
Figure 3.12 Radargram of the scan performed on 1/09/2008.....	23
Figure 3.13 Radargram of the scan performed on 4/7/2008.....	24
Figure 3.14 Average concrete thickness versus concrete age.....	25
Figure 3.15 GPR grid scan of the test driveway.....	26
Figure 3.16 Thickness measurement using extracted cores.....	26
Figure 3.17.....	27
Figure 3.18 Radargram of scan performed at the plate location.....	27
Figure 3.19 Radargram of scan performed at the T Sec. location.....	28
Figure 3.20 Radargram of scan performed at the right-side tie location.....	28
Figure 3.21.....	29
Figure 3.22 Movement of the left-side tie from its original location.....	30
Figure 3.23 Comparing thickness measurement using cores and GPR.....	31
Figure 4.1 GPR scan using SIR 3000 system on highway I-275.....	33
Figure 4.2 Radargram at Station 322 + 43.....	34
Figure 4.3 Radargram at Station 325 + 98.....	35
Figure 4.4 Radargram at Station 330 + 80.....	35
Figure 4.5 Grid setup at station 325 + 12.....	36
Figure 4.6 Grid used for scan # 1.....	37
Figure 4.7 Radargram of the x-direction scans (Scan #1).....	37
Figure 4.8 Radargram of the y-direction scans (Scan #1).....	38
Figure 4.9 Marked and detected locations of the metal ring on the grid of scan #1.....	38
Figure 4.10 Grid used for scan # 2.....	40
Figure 4.11 Radargram of the x-direction scans (Scan #2).....	40
Figure 4.12 Radargram of the y-direction scans (Scan #2).....	41
Figure 4.13 Marked and detected locations of the metal ring on the grid of scan #2.....	41
Figure 4.14 Location of the GPR scanned concrete pavement on Highway 30 in. Fremont, NE.....	43
Figure 4.15 Steel plate placed underneath the concrete pavement.....	44
Figure 4.16 Grid scan at the marked location of the steel plate.....	45

Figure 4.17 Radargram of the GPR grid scan at one station in field test # 3.....	45
Figure 4.18 Location of the GPR scanned concrete pavement on Hwy 2, Lincoln, NE.....	47
Figure 4.19 Placing reflector disks before paving Hwy 2.....	49
Figure 4.20 Grid scan at the marked location of the steel disk.....	49
Figure 4.21 Radargram (wiggle mode) of the GPR grid scan at plate # 15.....	50
Figure 4.22 Location of the GPR scanned concrete pavement on I-80, Lincoln, NE.....	52
Figure 4.23 Placing reflector disk before paving I-80.....	53
Figure 4.24 Grid scan at the marked location of the steel disk.....	54
Figure 4.25 Radargram (wiggle mode) of the GPR grid scan at plate # 14.....	54

List of Tables

Table 2.1 Relative permittivity of different material at a frequency of 1 GHz.....	6
Table 3.1 Number and dimensions of the metal objects used in lab test # 2.....	20
Table 3.2 Concrete Mix used in lab test # 2.....	21
Table 3.3 Results of GPR thickness measurments at different concrete ages.....	24
Table 3.4 Difference in thickness measurment usinf cores and GPR.....	30
Table 4.1 Stations and the corresponding core thickness.....	33
Table 4.2 Locations of plates scanned in field test #3.....	43
Table 4.3 Results of field test #3.....	46
Table 4.4 Locations of the 24 disks used in Hwy 2 project.....	48
Table 4.5 Results of field test #4a.....	51
Table 4.6 Results of field test #4b.....	51
Table 4.7 Locations of the 22 disks used in I-80 project.....	53
Table 4.8 Results of field test #5.....	56
Table 5.1 Benefit-Cost Comparison Between GPR and Corin.....	57

Acknowledgements

This project was sponsored by the Nebraska Department of Roads (NDOR) and the University of Nebraska-Lincoln. The support of the technical advisory committee (TAC) members is gratefully acknowledged. They spent a lot of time and effort in coordinating this project, discussing its technical direction, and inspiring the university researchers.

Acknowledgement also goes to the following undergraduate and graduate students who participated in the different tasks of the project:

1. Videgla Sekpe
2. Steve Cross
3. Regina Song
4. Michel Shafik
5. Catherine K. Armwood
6. Mary Naughtin
7. Kenzi Meyer
8. Eliya Henin

Disclaimer

This report was funded in part through grant[s] from the Federal Highway Administration [and Federal Transit Administration], U.S. Department of Transportation. The views and opinions of the authors [or agency] expressed herein do not necessarily state or reflect those of the U. S. Department of Transportation. The contents of this report reflect the views of the authors who are responsible for the facts and the accuracy of the data presented herein. The contents do not necessarily reflect the official views or policies of the Nebraska Department of Roads, nor the University of Nebraska-Lincoln. This report does not constitute a standard, specification, or regulation. Trade or manufacturers' names, which may appear in this report, are cited only because they are considered essential to the objectives of the report. The United States (U.S.) government and the State of Nebraska do not endorse products or manufacturers.

Abstract

Extracting concrete cores is the most common method for measuring the thickness of concrete pavement for construction quality control. Although this method provides a relatively accurate thickness measurement, it is destructive, labor intensive, and time consuming. Moreover, concrete cores are usually taken approximately every 750 ft, which may be inadequate for estimating the actual thickness profile of a pavement section; however extracting more cores would damage the pavement extensively and increase the labor cost and time excessively. Ground Penetrating Radar (GPR) is a well-established technique for subsurface exploration. Recently, GPR has been used for several transportation applications, such as measuring layer thickness in asphalt pavement, locating reinforcing bars and tendons, and detecting deteriorations and anomalies in concrete structures. The main advantages of GPR are speed, accuracy, and cost-effectiveness when scans are conducted on large areas.

The objective of this project is to investigate the accuracy and cost-effectiveness of using GPR for measuring the thickness of concrete pavement for quality assurance purposes. The GPR systems GSSI SIR20 and SIR3000 with a high resolution 1.6 MHz ground coupled antenna were used in measuring the thickness of concrete pavement up to 14 in. thick. Several laboratory and field tests were carried out to determine the accuracy of the GPR measurement at different concrete ages and when various metal artifacts are used underneath the concrete to improve the reflectivity of the bottom surface. Testing results indicated that GPR is cost-effective non-destructive technique for measuring the thickness of concrete pavement, compared to core extraction, and an accuracy of 1/8 in. can be achieved when appropriate reflectors and calibration cores are used.

Chapter 1 Introduction

Nebraska Department of Roads (NDOR) performs routine quality checks on their concrete pavement projects. This process is time consuming and costly endeavor with the current destructive method of coring. Therefore, a nondestructive, accurate, cost-effective, and speedy method can benefit the state. In this project, feasibility and accuracy of using Ground Penetrating Radar (GPR) for concrete pavement thickness quality assurance is studied through a systematic research methodology including review of literature, case studies testing various methodologies, and a cost-benefit analysis. Results of the study are presented in this report.

1.1 Background

Determining the thickness of concrete pavement is an important consideration for construction quality assurance of new pavements and structural capacity estimation of existing pavements. This information is essential for pavement management systems in order to maintain the safety, serviceability, and durability of pavement networks.

Currently, NDOR measures the thickness of concrete pavement using drilled cores and steel measuring devices. If the cores are in question, the ASTM C174 laboratory test method is adopted. Pavement cores are extracted every 750 ft and taken to the lab to determine the compliance of concrete construction with design specifications. The three-point calliper device shown in figure 1.1 is used to make length measurement at the center of the specimen and at eight additional points equally spaced along the circumference of the specimen (ASTM 2006a). The average of the nine measurements expressed to the nearest 0.1 in. is reported as the length of the concrete core.

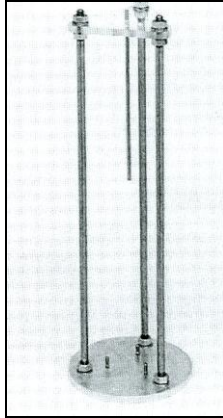


Figure 1.1 Core Measuring Apparatus

Although this procedure results in relatively accurate thickness measurements of concrete pavement, it provides local information as cores are required to be extracted every 750 ft. Therefore it is limited. In addition, core extraction is a time consuming, laborious, and destructive process. Moreover, the integrity of the pavement is already obstructed with the drilling and later-filling process.

1.2 Objectives

Given the drawbacks of the coring method discussed in the previous section, it is evident that a nondestructive alternative for pavement thickness measurements, which provides continuous information along the pavement section in a rapid and cost effective manner, can save NDOR time, money and provide the department with the possibility of continuous quality control on pavement contracts. The investigators propose that the GPR technology offers a solution to this need if a practical procedure overcoming the limitations is developed. Thus, the objectives of this research project are:

□ *General*

- Investigate the feasibility of using GPR on a routine basis for measuring the thickness of concrete pavement.

□ *Specific*

- Determine the accuracy of GPR in measuring the thickness of concrete pavement using “verification cores.”
- Investigate the effect of various parameters on GPR accuracy, such as pavement age and thickness.
- Identify the optimum number of “calibration cores” required to achieve the target accuracy.
- Evaluate the repeatability of GPR in thickness measurement.

Chapter 2 Literature Review

2.1 GPR Methodology

The GPR method involves the transmission of electromagnetic waves into the material under investigation. The reflections of these waves at interfaces and objects within the material are analyzed to determine the location (horizontal distance from a reference point) and depth (vertical distance from the surface) of the detected interfaces and buried objects. GPR can also be used to differentiate layers of material and to determine certain properties of the materials, such as their dielectric constants or conductivity for electromagnetic waves.

There are two basic types of radar waves: pulse and continuous wave. The pulse radar transmits a burst of radar energy and then waits for the energy (or echo) to be reflected back to the same antenna. The continuous radar wave, on the other hand, transmits a constant beam of energy that returns to a separate antenna when it meets a moving object (such as an aircraft or a car). The returned wave has a frequency that is slightly higher (if the object is moving toward the radar) or lower (if the object is moving away from the radar) than the frequency of the original wave. By measuring this change in frequency, the speed of the object can be determined.

GPR is the propagation of short pulse radar waves (pulse duration less than 1 ns) through the layers of materials under investigation. Figure 2.1 shows a radar signal that is emitted via an antenna into a structure composed of three different materials. Signals are reflected at the interfaces between the materials and their interfaces with the surrounding medium. Reflected signals are received by the same antenna to present one *scan* or *trace*. Several scans are taken at different locations on the investigated structure and their data are recorded in the storage device of the central unit. These data are then processed and displayed on a monitor for further analysis (manual or automatic interpretation). Analyzed GPR data can reveal significant information

about the materials within the structure (e.g. conductivity) and their condition (eg: layers and anomalies within the structure).

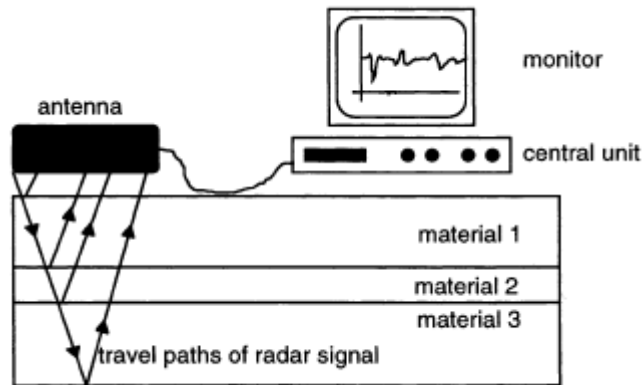


Figure 2.1 GPR Principles

From the electromagnetic standpoint, materials can be categorized as follows: a) metallic, and b) dielectric. Metallic materials have high conductivity and attenuate electromagnetic waves to a great extent resulting in shallow penetration, while dielectric materials have low conductivity and attenuate electromagnetic waves to a limited extent resulting in deep penetration. The relative dielectric constant of a particular material (ϵ_r , sometimes called relative permittivity) is the ratio of permittivity of the material to permittivity of vacuum ($\epsilon_0 = 8.854 \times 10^{-12}$ F/m). Although the transition from metallic to dielectric is gradual, this relative permittivity is used to indicate the nature of the material (high value for metallic and low value for dielectric). Table 2.1 lists the relative permittivity of different materials at an electromagnetic frequency of 1 GHz.

Table 2.1 Relative permittivity of different material at a frequency of 1 GHz (Table by GSSI, a major GPR manufacturer in the U.S.)

Material	Relative Permittivity
Air	1
Dry Masonry	3-5
Moist Masonry	5-26
Dry Concrete	5-8
Moist Concrete	8-16
Asphalt	3-5
Granite	5-7
Basalt	8
PVC	3
Water	81
Ice	4-8

The propagation velocity (v) of a transmitted radar signal through a material is a function of its relative permittivity (ϵ_r) and relative magnetic permeability (m_r) as follows:

$$v = \frac{c}{\sqrt{\epsilon_r m_r}} \quad (2.1)$$

In low-loss materials, as in most of the dielectric materials, the relative magnetic permeability (m_r) can be assumed to be unity. Therefore, if the relative permittivity of the material under investigation is known, the propagation velocity can be calculated using Equation 2.1. The propagation velocity of the waves within specific materials is then used to determine the thickness of each material layer using the two-way travel time recorded by the GPR antenna. The difference in time between the reflected signals at the top and bottom interfaces of the layer times the velocity gives the distance traveled by the wave, i.e. the thickness of the layer. It should be noted that relative permittivity of a material is frequency-dependent and is influenced by several parameters, such as the temperature, moisture, and salt content of the material. These

parameters have to be considered through calibration before calculating the velocity in order to obtain accurate thickness measurements.

When the incident signal meets the interface between two materials with different dielectric constants, part of the incident energy is reflected, while the other part is transmitted. The amount of reflected and transmitted energy is determined by the reflection and transmission coefficients (R and T) respectively. These coefficients are dependent on the relative impedance of the two materials (z_{r1} , z_{r2}), which are functions of the dielectric constant of the materials (ϵ_{r1} , ϵ_{r2}). These coefficients are calculated as follows:

$$R = \frac{z_{r2} - z_{r1}}{z_{r2} + z_{r1}} \quad (2.2)$$

$$T = 1 - R \quad (2.3)$$

$$z_r = \sqrt{\frac{m_o}{\epsilon_o \epsilon_r}} \quad (2.4)$$

where $m_o = 4\pi * 10^{-7}$ H/m is the magnetic permeability of free space.

As can be deduced from equations 2.2, 2.3, and 2.4, the smaller the difference in the dielectric constant of the two materials, the smaller the reflection coefficient and the larger the transmission coefficient. This means that the change of amplitude of the energy (i.e. attenuation) reflected from the interface between two materials is a good indicator of the properties of these materials. As the incident energy continues to penetrate other materials and meets successive interfaces, other reflections are sent back to the antenna and recorded over time to generate the

waveform. Measuring the time and amplitude of reflections (peaks or valleys) in the waveform facilitates the determination of layer thicknesses (eq. 2.1), depth of buried objects, and changes in material properties (eq. 2.2, 2.3, and 2.4), which are the basic purposes of using the GPR technology.

2.2 Use of GPR for Pavement Layer Thickness Measurements

Traditionally, highway engineers use drilled cores to obtain pavement samples to perform laboratory testing to determine the thickness of different layers, examine the conditions that may cause pavement deterioration, and select the most appropriate maintenance actions. Conventional methods of core sampling are expensive and time-consuming because they are labor intensive and require lane closure until all cores are drilled, checked and refilled, which affects the safety of workers and the traveling public (Federal Highway Administration 2004).

GPR has been used for a variety of applications relating to pavement evaluation, such as determining pavement thickness, locating changes in pavement structure, detecting voids under jointed concrete slabs, identifying location and orientation of dowels in jointed concrete pavement, and spotting moisture and stripping within asphalt pavement (Maser 1996).

Several studies have been reported on using GPR to measure the thickness of pavement layers. Loulizi *et al.* (2003) conducted an experiment on a 150 meter long asphalt paved secondary road and reported an error percentage of less than 3.6% between the measured thickness and the GPR-predicted thickness. Al-Qadi and Lahouar (2004) conducted a GPR survey over a 40 meter long asphalt pavement section at the Virginia Smart Road and reported an average layer thickness error of 2.9% compared to core thickness. Willett *et al.* (2006) conducted a study to evaluate the accuracy of GPR in measuring pavement layer thickness in

both asphalt and concrete pavement. This study showed a significant increase in GPR accuracy by increasing the number of calibration cores in asphalt and concrete pavement.

GPR surveys have also been used to control the embedded depth and the inclined position of the dowels or anchors that are placed perpendicular to the transverse and longitudinal joints in concrete pavements during construction (Maierhofer 2003). Dowel positioning errors result in irregular concrete cracks and rapid joint deterioration. Figure 2.2 shows the GPR waveform recorded using 1.5 GHz antenna close to a transverse joint. This information is interpreted and used to locate each dowel and enabled quality control in pavement construction. Data interpretation requires training, which is available by the GPR manufacturers with the purchase of their equipment. In-house training and practice is also beneficial, where the operators scan test specimens with known objects/layers and confirm the known variables with the scan data.

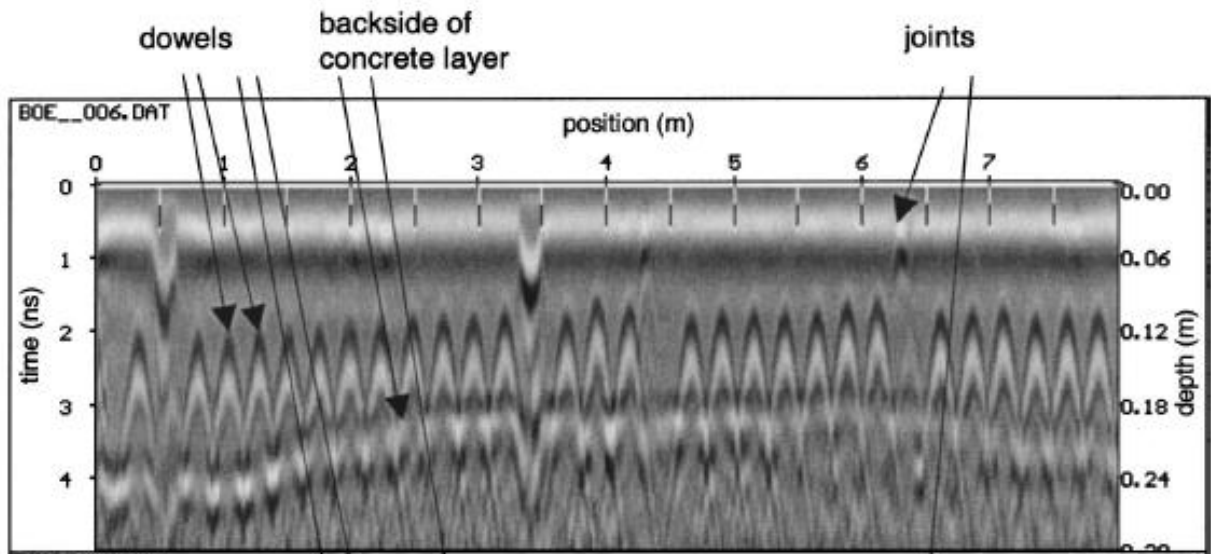


Figure 2.2 GPR survey of concrete pavement (Maierhofer 2003)

Several techniques are available to estimate pavement thickness using GPR for the Department of Transportation. Antennas can be used in two ways, air coupled and ground

coupled. An air coupled antenna unit can be mounted to the back of a moving vehicle and travel at high speeds with the antenna between six and twenty inches above the pavement which does reduce the depth of penetration. A ground coupled system antenna rests completely on the ground and reduces the reflection from the top of the concrete, therefore increasing the depth of penetration but reduces the speed of collection. Equation 2.5 can be used to estimate the thickness of the pavement.

$$d_i = \frac{ct_i}{2\sqrt{\epsilon_{r,i}}} \quad (2.5)$$

Where d_i = the thickness of the layer

t_i = the two way travel time of the signal through the layer

c = the speed of light

$\epsilon_{r,i}$ = the dielectric constant of the layer

Using this equation the dielectric needs to be found using the calibration technique built into the GPR and a strong reflection below the layer of concrete, possibly a metal plate that will reflect all of the signal energy back to the antenna. This technique can also be applied to pavement with multiple layers with slightly more complicated analysis. When Al-Qadi tested this technique during thickness measurements of hot mix asphalt layers, an error of 2.9% compared to measured core samples was recorded (Al-Qadi 2004).

A presentation at the Eighth International Conference on Ground Penetrating Radar described the use of vehicle mounted radar scans as promising in both accuracy and speed of collection where data is collected using two air-launched 1 GHz antennas suspended off of the rear of a vehicle bumper. This system is calibrated by placing an aluminum plate on the surface of the ground and then starting the radar system recording and driving away only after several

scans have been recorded. The model also assumes a smooth surface and homogenous pavement. The accuracy of this method is better than commonly encountered in ASTM D3549 through coring and ASTM D4748 by short-pulse radar (Olhoeft 2000).

In a study conducted in Kentucky, the accuracy of thickness measurement using GPR on asphalt and concrete using a 1 GHz air launched horn antenna was measured in a variety of environments. The relationship was then evaluated between data analyzed with and without core samples taken. This study recommends the use of core samples to increase the accuracy of depth measurement by using the core depths to calibrate the ground penetrating radar. Four core samples is recommended to minimize the error of the ground penetrating radar, but it does not mention what length or area of concrete this number of cores is based on. Overall, it is concluded that any addition of core samples to the GPR has a positive effect on the accuracy of the scans. For concrete slabs the accuracy ranges between 1.66 inches and 0.01 inches for pavement thicknesses of 9 to 12 inches (Willet 2006).

A project for the Florida Department of Transportation was carried out to further develop GPR techniques and capabilities to increase accuracy and to reduce post-processing and operator interaction. A computer program named *Thickness Evaluation of Roads by Radar* (TERRA) was developed to automate the GPR process. Using this program and an air coupled antenna radar vehicle showed a resulting error of only 0.30 inches compared to core samples (Kurtz 2001).

Research has been done utilizing many different types of GPR and post-processing techniques to accurately measure the thickness of pavement by Al-Qadi *et al.* in 2001. They used GPR to accurately measure the thickness of flexible pavement by calibrating the GPR at each location through the use an aluminum sheet placed below grade. Two GPR systems were used simultaneously, air-coupled and ground-coupled collected at 16 kph and 1 scan per 110 mm.

Cores were taken to verify the data with the average error being only 6.7%. Maser in 1996 measured as-built conditions of pavement using GPR and PAVLAYER software with an accuracy of $\pm 7.5\%$. Mesher *et al.* (1995) reported a project where a GPR system called “Road Radar” was used to measure pavement thickness on three sites. The self calibrating system was used with a 2.5 GHz antenna. Linear regression statistical analysis was used reporting an average R^2 value greater than 0.9 (Loulizi 2003).

The principal investigators (PIs) of this project also carried out some relevant work before the granting of the current project. An exploratory study was carried out by the PI using the Structure Scan system to accurately measure the cover thickness in reinforced concrete slabs and to precisely locate reinforcing bars. Figure 2.3 shows five 3 ft x 3 ft slabs with thickness ranging from 6 inches to 12 inches prepared for testing at the Structures Laboratory at Peter Kiewit Institution (PKI) in Omaha, Nebraska. Results of this study are shown in Appendix A.



Figure 2.3 Reinforced Concrete Slabs Used for GPR Testing at PKI labs by authors

Chapter 3 Laboratory Tests

Two laboratory tests were carried out to estimate the accuracy of measuring the thickness of concrete pavement using GPR and to determine the most economical way to improve this accuracy. The next two subsections describe the two tests in details.

3.1 Lab Test # 1

The first lab test was performed on September 20, 2007 at the PKI Structural Laboratory, where the temperature is approximately 75°F and the relative humidity is approximately 70%. In this test, a 3 ft x 3 ft x 12 in. reinforced concrete slab was placed on top of 8 in. thick base layer made of 47B sand and gravel. The concrete of this slab is almost one and a half years old and its dielectric constant is assumed to be 6.25.

A 2 in. diameter metal ring was placed on the base layer as shown in figure 3.1 before placing the concrete slab. A 2 ft x 2ft grid was placed on the top surface of the slab and two GPR grid scans were performed at 2 in. spacing as shown in figure 3.2.



Figure 3.1 Metal ring placed underneath a 12 in. thick concrete slab



Figure 3.2 GPR grid scan of the 12 in. thick concrete slab

Figure 3.3 shows the plan, side view and elevation of the 12 in. thick reinforced concrete slab and the location of the metal ring. The slab had a 4 in. deep saw cut at the middle and was reinforced with two #8 bars crossing the cut to simulate the dowel bars across the joints in concrete pavements.

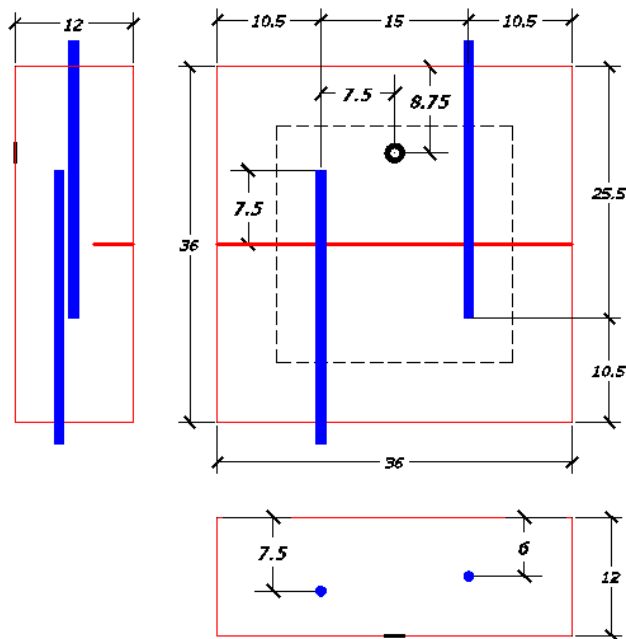


Figure 3.3 Projection views of the tested slab

The first grid scan was performed on Thursday, September 20, 2007. Figure 3.4 shows the grayscale presentation of the GPR signal reflections for a part of the grid scan. The vertical axis represents the depth through the concrete slab in inches, while the horizontal axis represents the distance along the scanned lines. The zero point on the vertical axis means the top surface of the slab. Each mark on the vertical axis represents a half inch measurement, while each mark on the horizontal axis represents a one foot measurement. Since all the grid lines have the same in length of 2 feet every two marks on the horizontal axis represents one line on the scanning grid. Figure 3.4 shows that reinforcing bars were clearly detected at $y = 20$ in. as indicated by the strong parabolic reflections enclosed in the green oval, while the metal ring was poorly detected at the same location as indicated by the weak parabolic reflection enclosed in the red circle. Similar reflections were also detected at parallel scan lines ($y = 18$ in., and $y = 22$ in.).

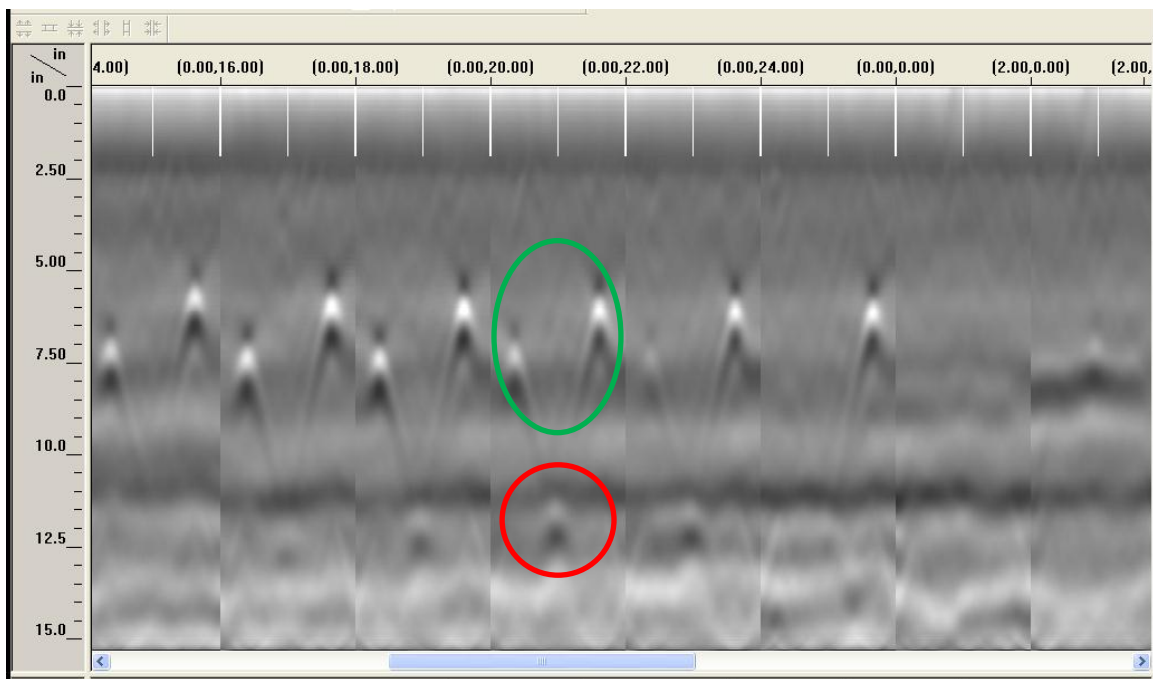


Figure 3.4 GPR single reflections at the reinforcing bars and metal ring

The second grid scan was performed on November 5, 2007 on the same grid used in the first scan. In this scan, a 3 foot long metal strip that was 2 in. wide and 1/4 in. thick was inserted underneath the concrete slab parallel to the x axis (i.e. perpendicular to the reinforcing bars) at $y = 8$ in. Figure 3.5 shows the grayscale presentation of the GPR signal reflections for a part of the grid scan. It also shows that reinforcing bars were clearly detected at $y = 20$ in. as indicated by the strong parabolic reflections enclosed in the green oval, while the metal ring was poorly detected at the same location as indicated by the weaker parabolic reflection enclosed in the red circle. The metal strip was also clearly detected at $x = 0$ as indicated by the strong parabolic reflections enclosed in the yellow circle. By comparing these reflections, it can be concluded that the strength (i.e. amplitude) of the reflected signals is directly proportional to the surface area of the detected metal object.

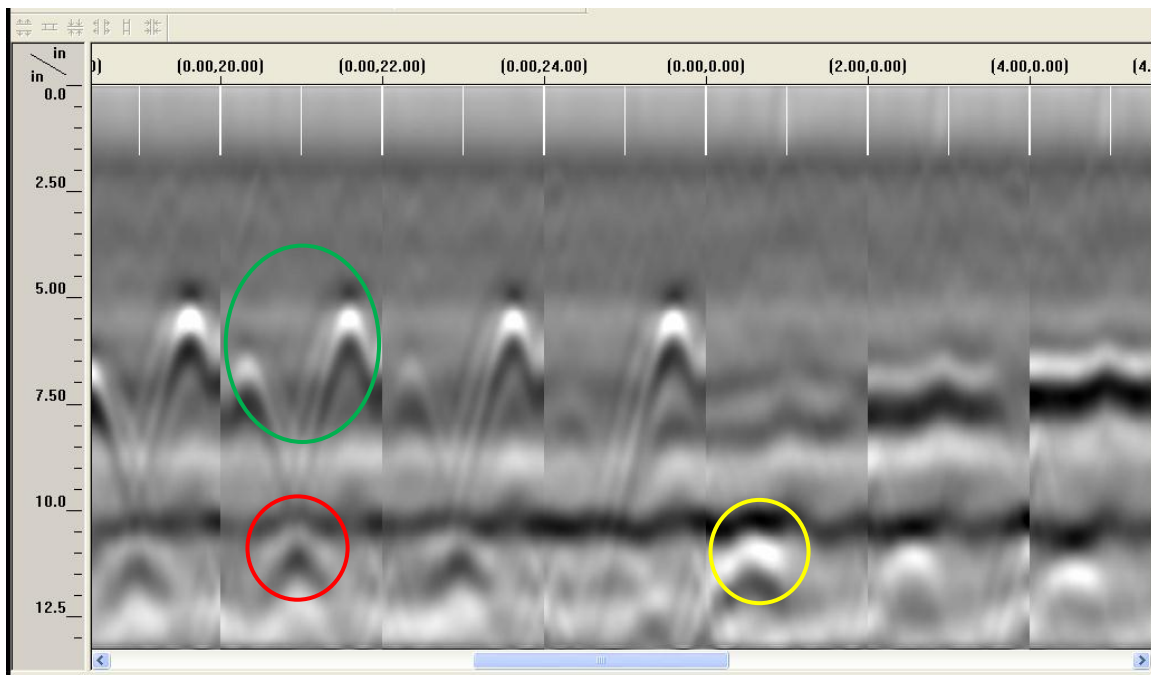


Figure 3.5 GPR signal reflections at the reinforcing bars, metal ring, and metal strip

A third scan was performed on November 6, 2007 on the same concrete slab but using the line scan instead of the grid scan. In this scan, a 20 in. long, 3/4 in. wide, and 1/8 in. thick form tie, as shown in figure 3.6, was inserted parallel to, and in between the two reinforcing bars. Figure 3.7 shows the grayscale presentation of the GPR signal reflections for a part of the line scan. This figure shows that reinforcing bars were clearly detected as indicated by the strong parabolic reflections enclosed in the green circle, while the form tie was less clearly detected as indicated by the weaker parabolic reflection enclosed in the yellow circle. By comparing the two reflections, the previous conclusion that the strength of the reflected signals is highly dependent on the object surface area is confirmed.



Figure 3.6 Form ties used in the lab test # 1

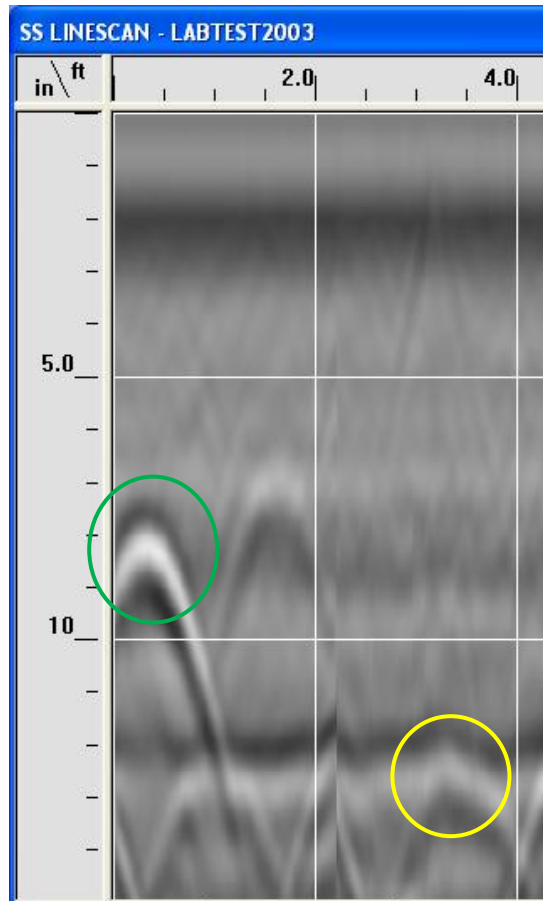


Figure 3.7 GPR signal reflections at the reinforcing bars and form tie

3.2 Lab Test # 2

The second lab test was performed on a 14ft x 12ft concrete driveway that was built specifically for research purposes. The driveway was built at one of the University of Nebraska-Omaha facilities that are located at the south campus. The specific location of the driveway is indicated by the red rectangle in the map shown in figure 3.8. The objective of this lab test is threefold:

- 1- Estimate the accuracy of GPR in measuring the thickness of concrete pavement.
- 2- Evaluate the effectiveness of using different metal objects from the constructability and thickness measurement accuracy point of view.
- 3- Determine the effect of the concrete age on thickness measurements using GPR.

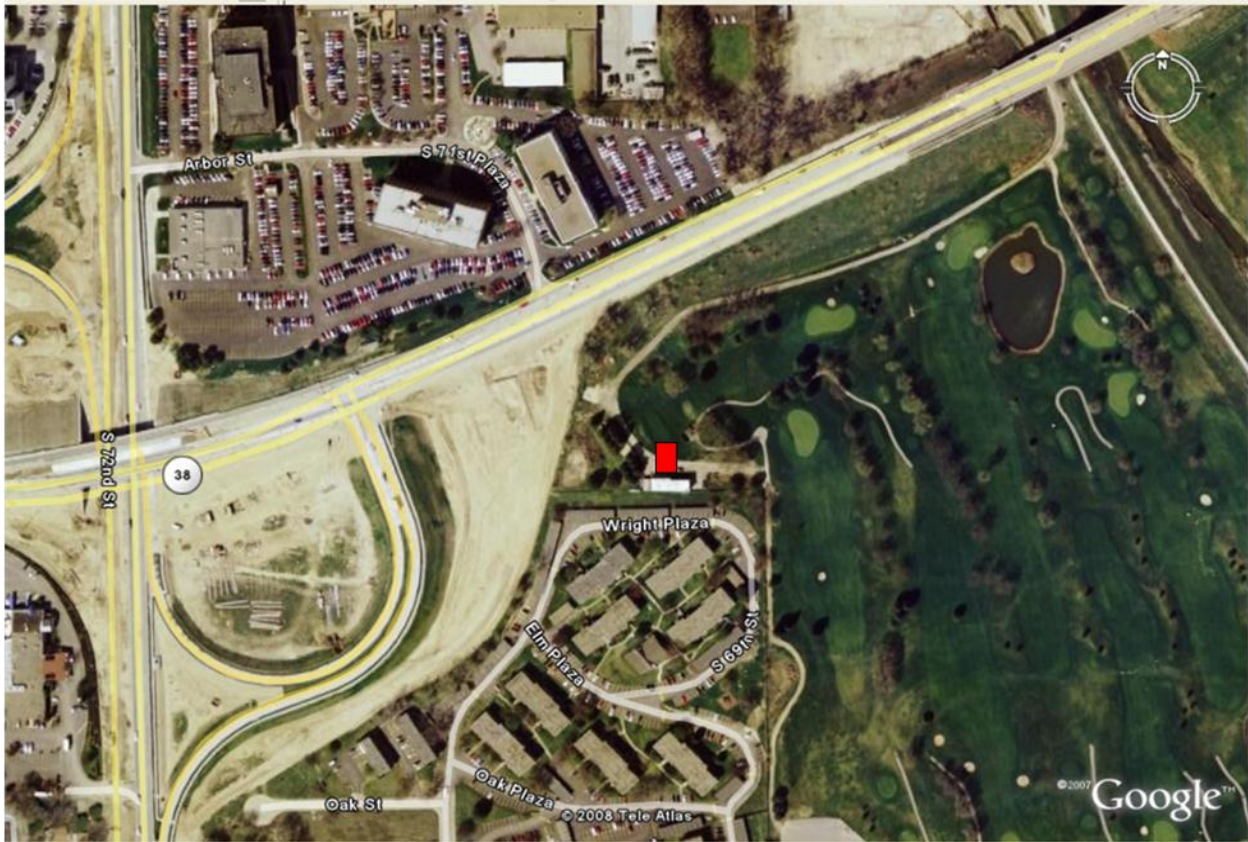


Figure 3.8 Location of the driveway built for lab test # 2

Based on the results of the lab test # 1, five metal objects were chosen for the lab test # 2. These objects are shown in figure 3.9 and listed in table 3.1



Figure 3.9 The five metal objects used in lab test # 2

Table 3.1 Number and dimensions of the metal objects used in lab test # 2

Object	Number	Dimension (in.)
T Sec.	1	1.5 x 1.5 x 33
L Sec.	1	1 x 1 x 34
Form Tie	2	20 x 3/4 x 1/8
Plate	1	6 x 6 x 1/8

The construction of the driveway started on November 19, 2007 by leveling the subgrade through cut and fill operations using the existing soil and 47B sand and gravel. The subgrade was leveled so that the thickness of the concrete pavement varies from 10 in. to 14 in. Then, three sides of the driveway were formed using 2 x 12 lumbers, while the fourth side was formed by the side of an existing driveway that is 14 in. thick. On December 3, 2007, the subgrade was compacted using a mobile compactor and the five objects listed in table 4.1 were anchored to the subgrade at the locations shown in figure 3.10. It should be noted that the top of the figure is pointing toward the south. On December 4, 2007, the concrete was poured, vibrated, finished, and covered with foam planks for curing. Table 3.2 lists the design of the concrete mix used in this application, which is one of the Nebraska Department of Roads (NDOR) standard mixes specified for pavement construction. Photos of the various construction steps are provided in Appendix A.

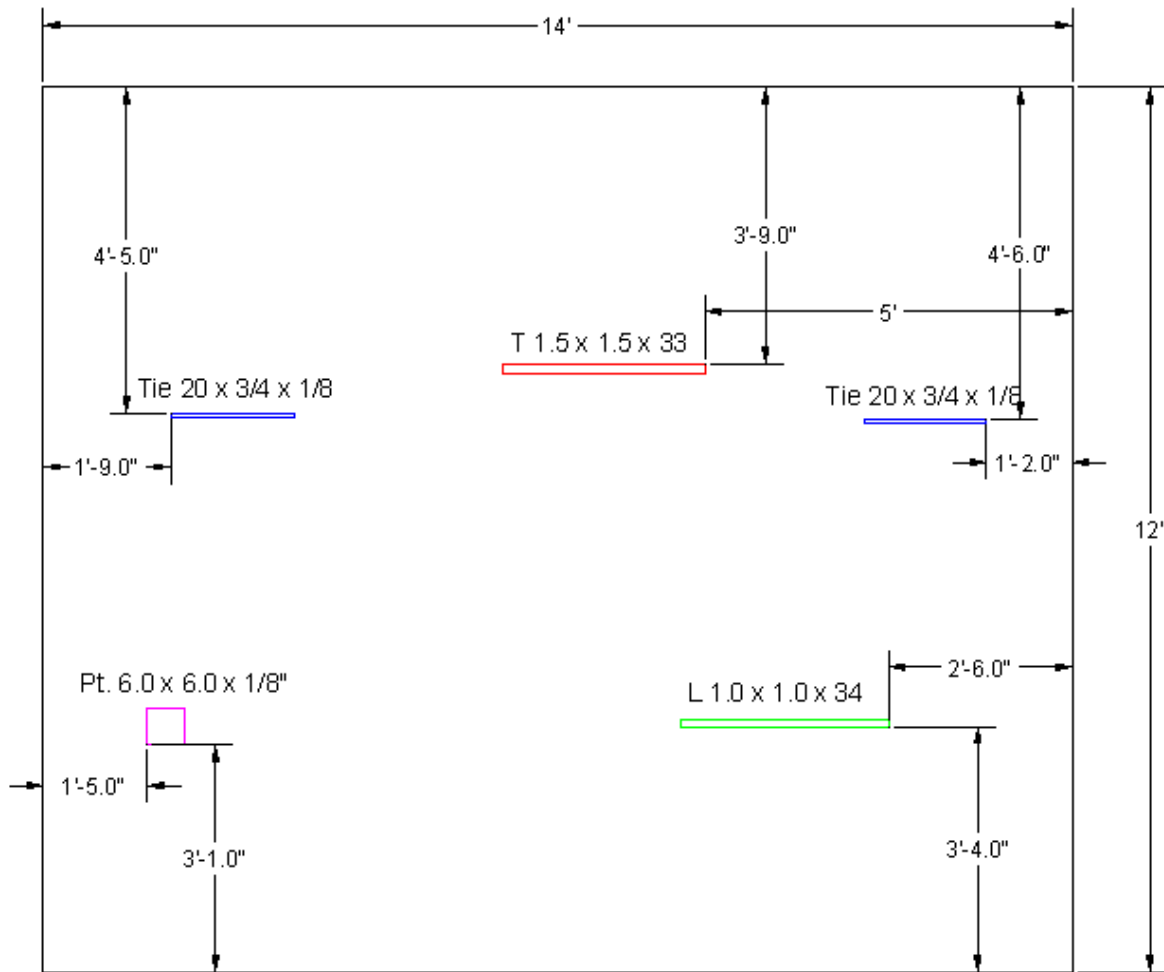


Figure 3.10 Location of the five metal objects used in lab test # 2

Table 3.2 Concrete Mix used in lab test # 2

Concrete Mix	
Component	lb/cy
Cement IPF	564
47 B Sand	2191
3/4" Limestone	939
w/c Ratio	0.4
Water	226

In order to investigate the effect of concrete age on the thickness measurement using GPR, several scans were taken at different times. These scans were taken using identical settings for the GPR equipment, data processing procedures, and scanning location to eliminate the impact of any parameter other than the concrete age. Dielectric constant was assumed to be 6.25, which corresponds to that of a dry concrete. Figures 3.11, 3.12, and 3.13 show snapshots of the radargrams obtained from the grid scans of the concrete driveway at the T-Sec. location at three different times. The clear hyperbolas appeared on these radargrams indicate strong signal reflections, which results in accurate thickness measurements. Five readings were taken from each radargram to estimate the average concrete thickness at the scanned location. These values are listed in table 3.3 along with their average and the age of the concrete at the time of scan. Figure 3.14 shows a plot of these values versus the concrete age in days and the straight line that best fits the data points. This plot indicates that there is a strong correlation (coefficient of determination is 83%) between the measured depth of the embedded object and the age of the concrete; the older the concrete, the smaller the measured thickness (0.01 in. per day). This is mainly due to the fact that the older the concrete, the drier it becomes and, the closer its actual dielectric constant gets to the assumed value, which affects the signal velocity in concrete.

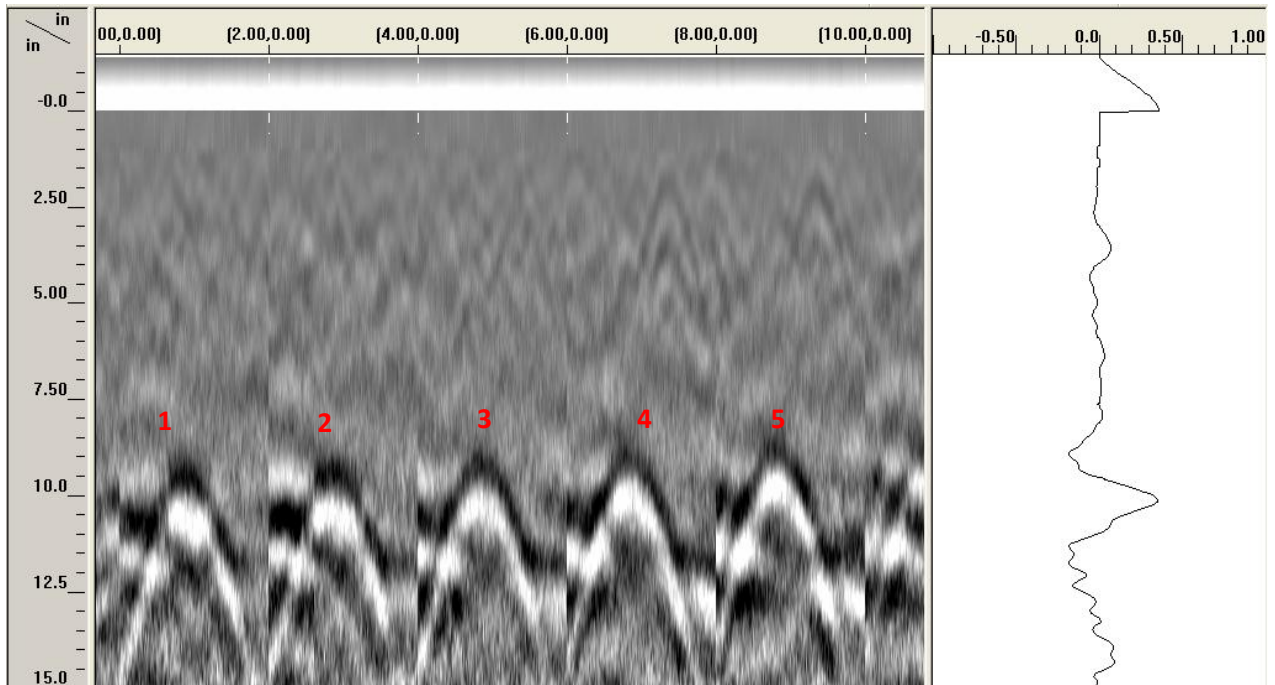


Figure 3.11 Radargram of the scan performed on 12/21/2007

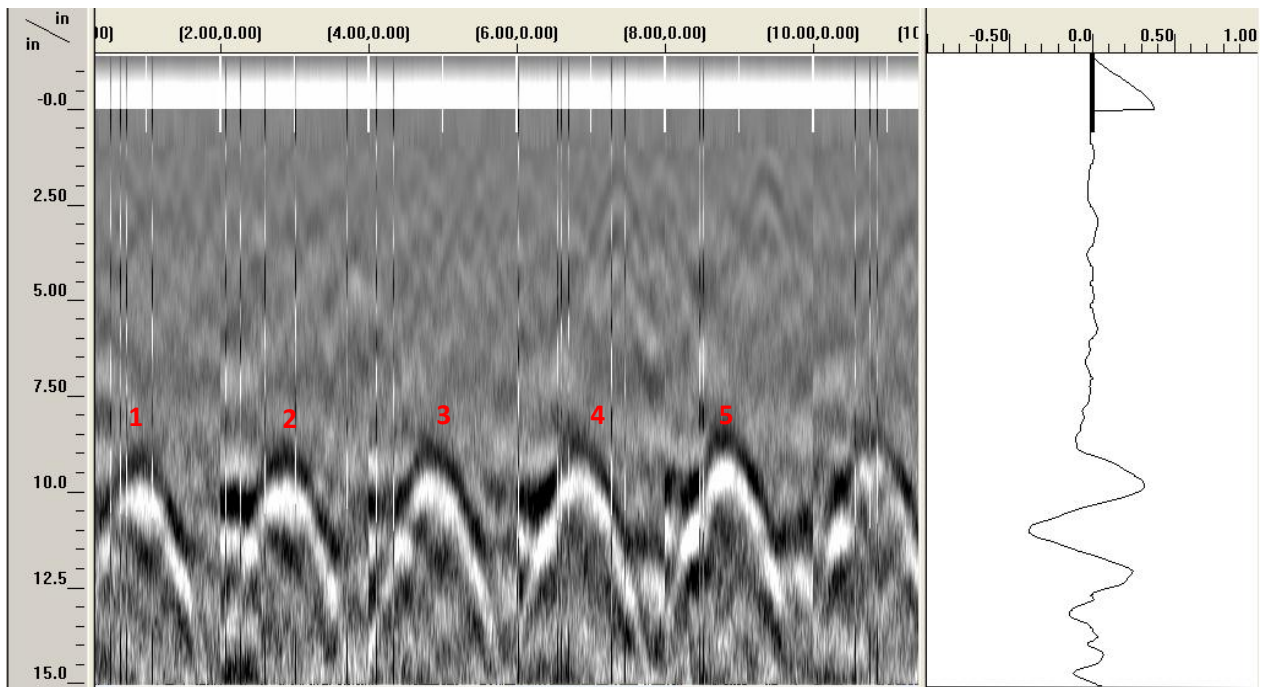


Figure 3.12 Radargram of the scan performed on 1/09/2008

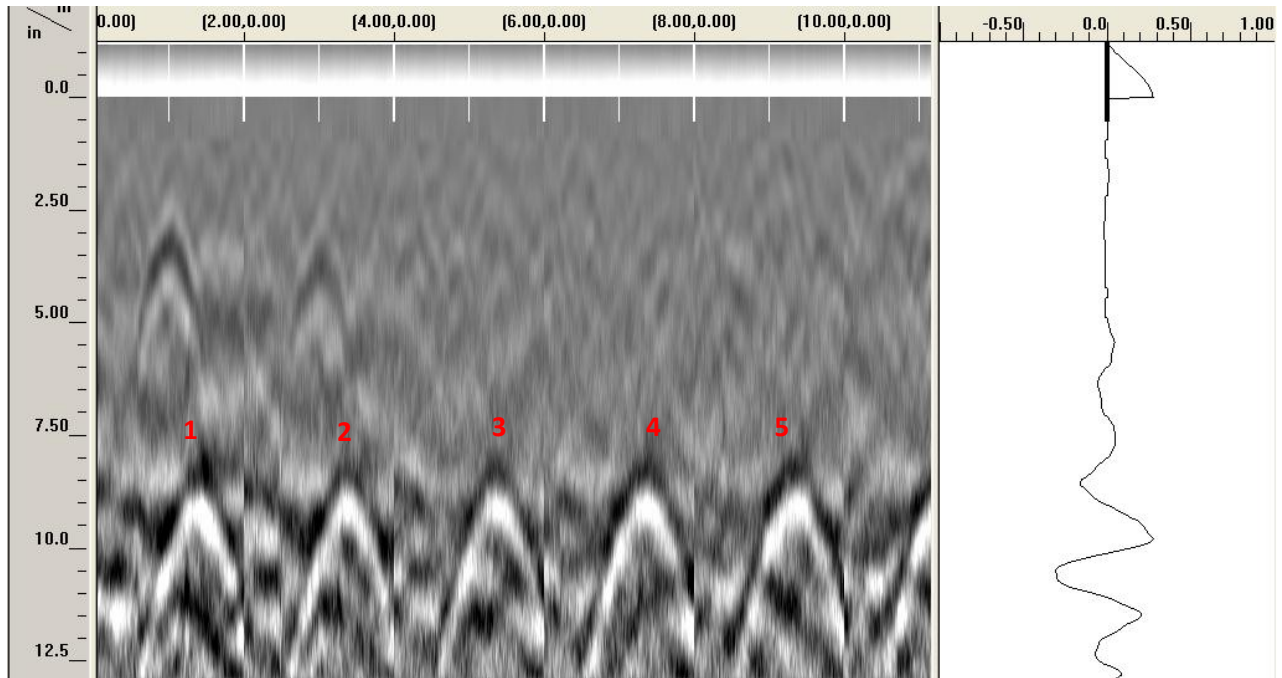


Figure 3.13 Radargram of the scan performed on 4/7/2008

Table 3.3 Results of GPR thickness measurements at different concrete ages

Construction Date		Reading Number					Average Thickness (in)
Test Date	Concrete Age (day)	1	2	3	4	5	
12/21/2007	17	10.5	10.4	10.2	10.1	9.8	10.2
1/9/2008	36	10.3	10.2	9.9	9.8	9.7	10.0
4/7/2008	125	9.2	9.1	9.1	9.2	9.0	9.1

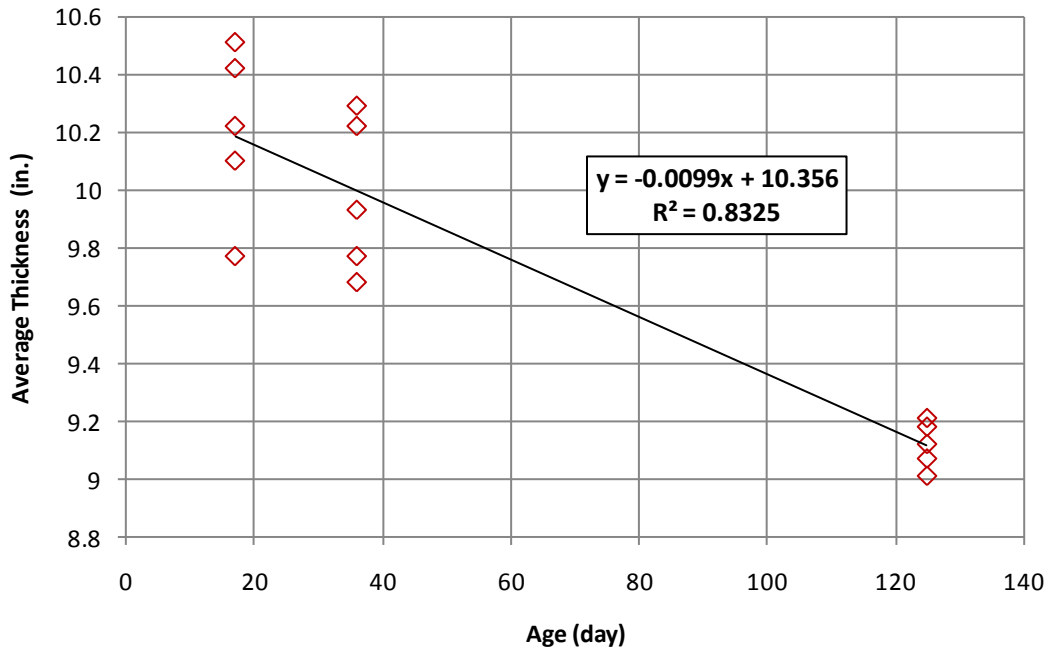


Figure 3.14 Average concrete thickness versus concrete age

In order to determine the accuracy of concrete thickness measurement using GPR, grid scans were performed on the top surface of the test driveway at the location of the five metal objects on May 1, 2008 as shown in figure 3.15. Five 6 in. diameter cores were extracted on the same day at the locations of the five objects. Three different thickness measurements were taken from each core as shown in figure 3.16 to determine the average concrete thickness. Grid scans were performed using identical equipment settings and processed using identical procedures to ensure data consistency and reliability. Figures 3.17, 3.18, 3.19, 3.20, and 3.21 show snapshots of the radargrams obtained from the grid scans at the locations of the five metal objects.



Figure 3.15 GPR grid scan of the test driveway



Figure 3.16 Thickness measurement using extracted cores

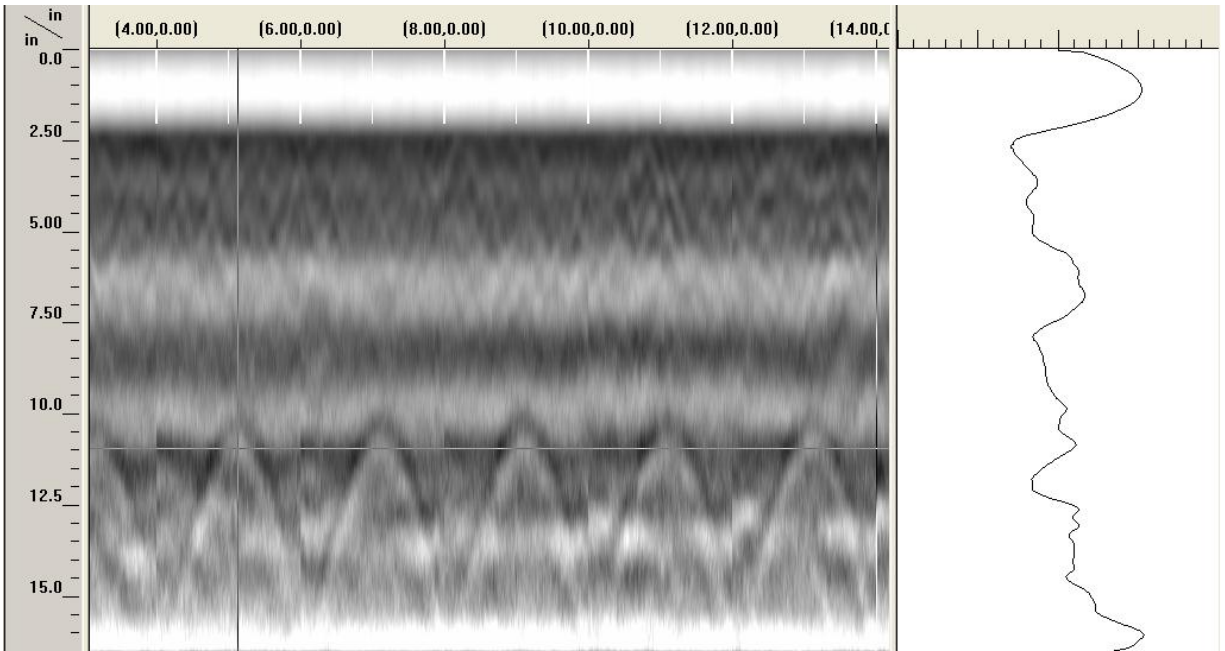


Figure 3.17 Radargram of scan performed at the L Sec. location

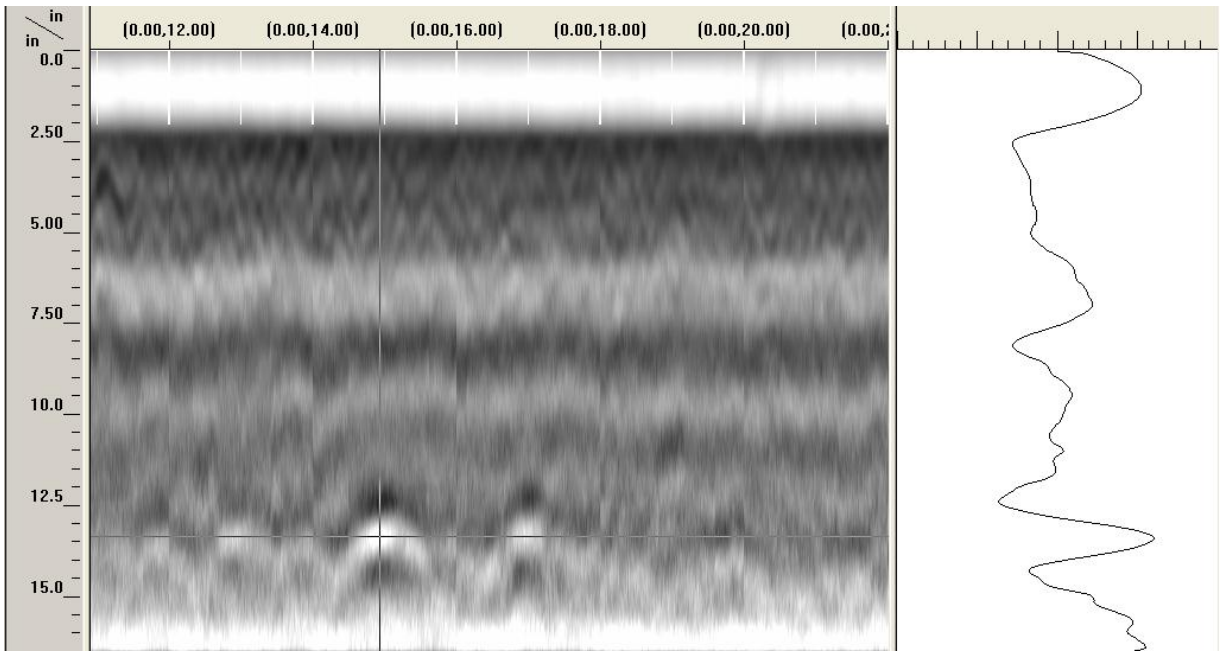


Figure 3.18 Radargram of scan performed at the plate location

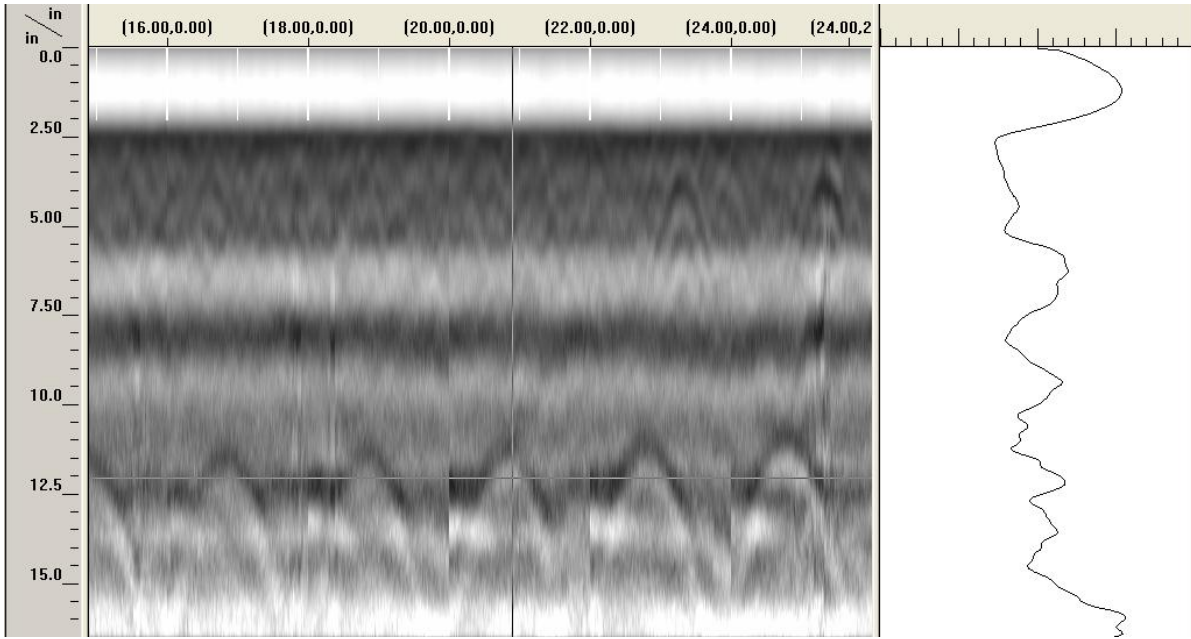


Figure 3.19 Radargram of scan performed at the T Sec. location

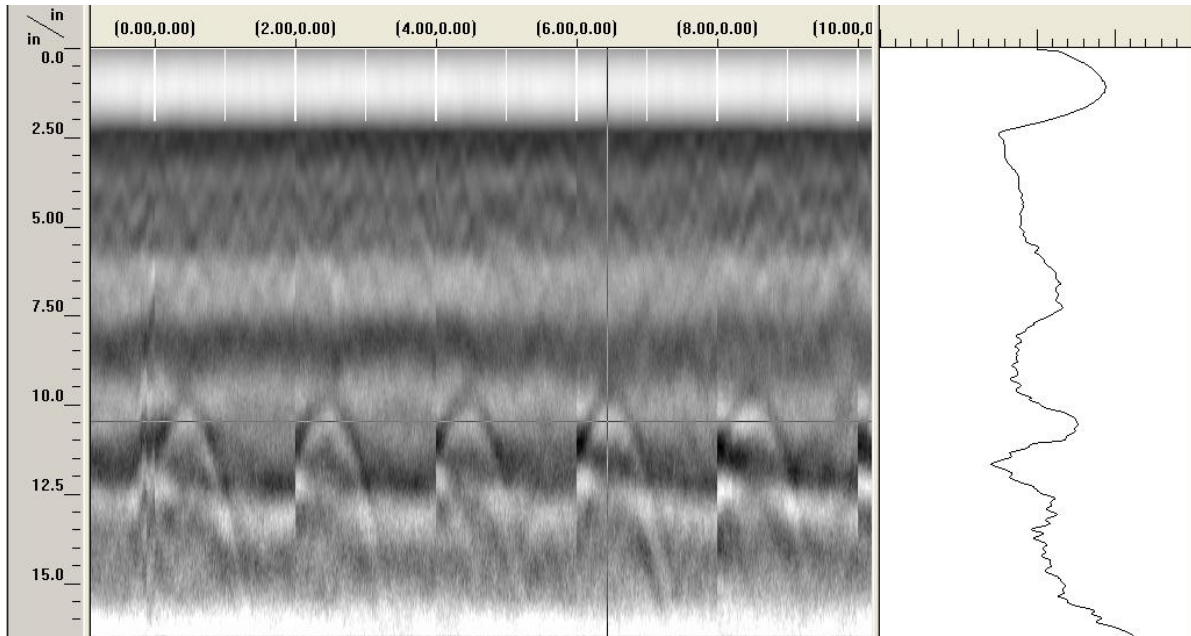


Figure 3.20 Radargram of scan performed at the right-side tie location

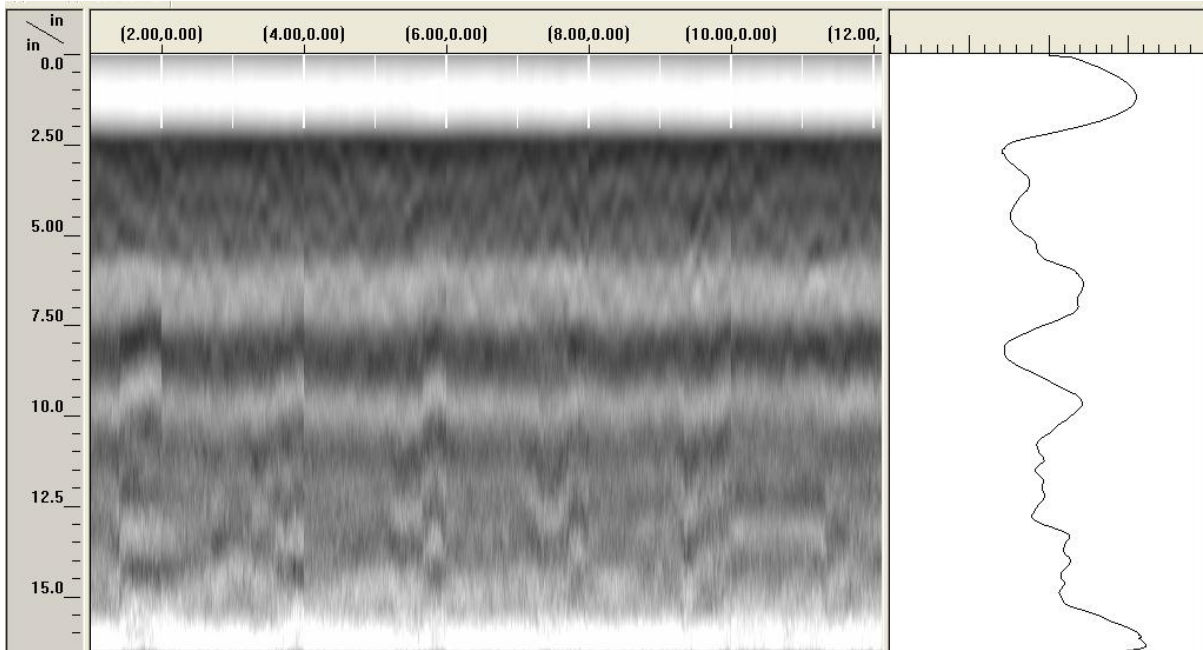


Figure 3.21 Radargram of scan performed at the left-side tie location

All the previous radargrams, except figure 3.21, show clear hyperbolas that indicate strong signal reflections and accurate detection of the metal objects. Figure 3.21 shows a very poor detection of the left-side tie, which resulted in not being able to determine the concrete thickness at that location using GPR. This was basically due to the movement of the left-side tie from its original location during concrete pouring and vibration. This fact was revealed when the core was extracted at that location and the tie appeared to be shifted and rotated as shown in figure 3.22.



Figure 3.22 Movement of the left-side tie from its original location

Several readings were taken from each radargram to estimate the average concrete thickness at the four scanned locations. Table 3.4 lists the average concrete thickness as measured by GPR and the corresponding actual concrete thickness as measured from the extracted core. The differences between the two values are presented in inches and as percentages from the actual thickness. These differences indicate that GPR can provide concrete thickness measurement with accuracy up to 1/8 of an inch, which is approximately 1.5%. Figure 3.23 also shows a plot of these values side by side for each of the metal objects.

Table 3.4 Difference in thickness measurement using cores and GPR

Item	Core Measurement	GPR Measurement	Difference (in)	Difference (%)
T Sec.	11 1/8	11	1/8	1.1%
L Sec.	10 1/8	10	1/8	1.2%
Tie R	9 3/4	9 1/2	2/8	2.6%
Tie L	13 1/8	N/A	N/A	N/A
Plate	12 1/4	12 3/8	1/8	1.0%
Average Difference (in)			1/8	1.5%

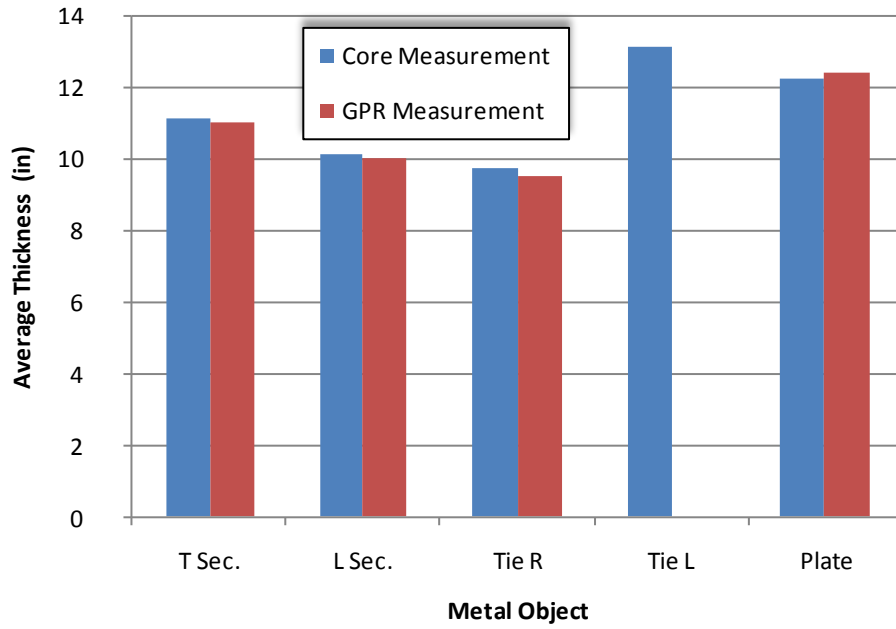


Figure 3.23 Comparing thickness measurement using cores and GPR

Chapter 4 Field Test

Three field tests were carried out to investigate the feasibility and reliability of using GPR for measuring the thickness of concrete pavement. Information obtained from the laboratory tests presented in the previous section was used to guide field applications. Below is the full description of each field test.

4.1 Field Test # 1

The first field test was performed on Friday, September 14, 2007 from 11:00 a.m. – 1:30 p.m. at Highway I-275 outside of Hooper and Fremont, NE. NDOR was investigating problems on that project and took several cores at the locations shown in table 1. Therefore, it was a good place to evaluate the accuracy of GPR against actual cores. The temperature was 55°F and the test was attended by NDOR staff members as well as University of Nebraska-Lincoln (UNL) faculty members and graduate students. Ten stations were scanned where cores were taken. Table 4.1 lists the stations and the core thickness as provided by NDOR. The 1.5 GHz ground-coupled antenna was used with the SIR 3000 GPR system mounted on a mobile cart as shown in figure 4.1. Line scans using concrete scan mode were performed over the location of the extracted cores after filling them with grout. Each scan was approximately 20 ft long, 10 ft before and 10 ft after the core location. Sampling rate was set to 200 scans per second, which results in approximately 60 scans per linear foot.

Table 4.1 Stations and the corresponding core thickness

Station	Core Thickness (in.)
322 + 43	10.2
325 + 98	14.1
326 + 40	11.6
327 + 20	11
328 + 99	10.7
330 + 80	10.6
330 +57	10.9
328 + 17	10.7
324 + 70	10.9
325 + 12	11.4



Figure 4.1 GPR scan using the SIR 3000 system on Highway I-275

Figures 4.2, 4.3, and 4.4 show radargrams snapshots from the scanning of three different stations. These figures also show the locations of the bottom surface of the concrete at these stations. These radargrams indicate that GPR signal reflections at the bottom surface of the concrete are weak and unclear, which make the surface detection difficult and thickness

measurement inaccurate. Based on thickness measurement obtained from the extracted cores, the RADAN software was used to re-calculate the dielectric constant of the concrete. The dielectric value that made the depth of the bottom surface of the concrete obtained from GPR signal reflections match the actual pavement thickness was determined for each station. These values were found to be substantially different from each other and some of them were slightly higher than the standard range of conventional concrete (between 4 and 11). Therefore, it was concluded that it is highly recommended to use metal objects at the interface between the concrete pavement and its base layer. This will help producing strong reflections at the bottom surface of the concrete that can be easily identified and used for more reliable thickness measurements.

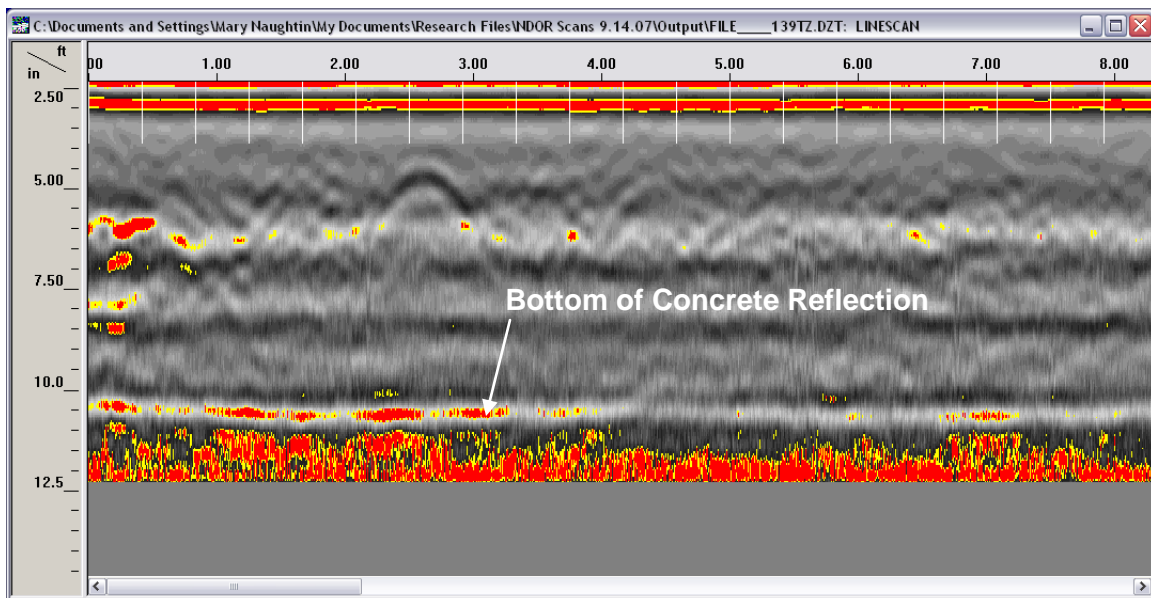


Figure 4.2 Radargram at Station 322 + 43

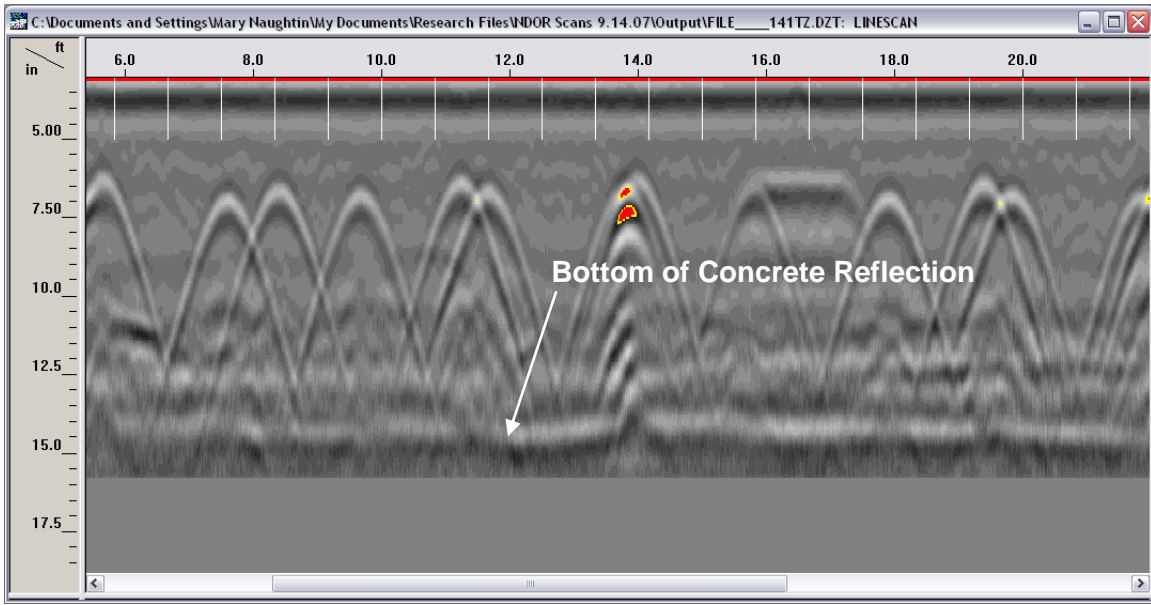


Figure 4.3 Radargram at Station 325 + 98

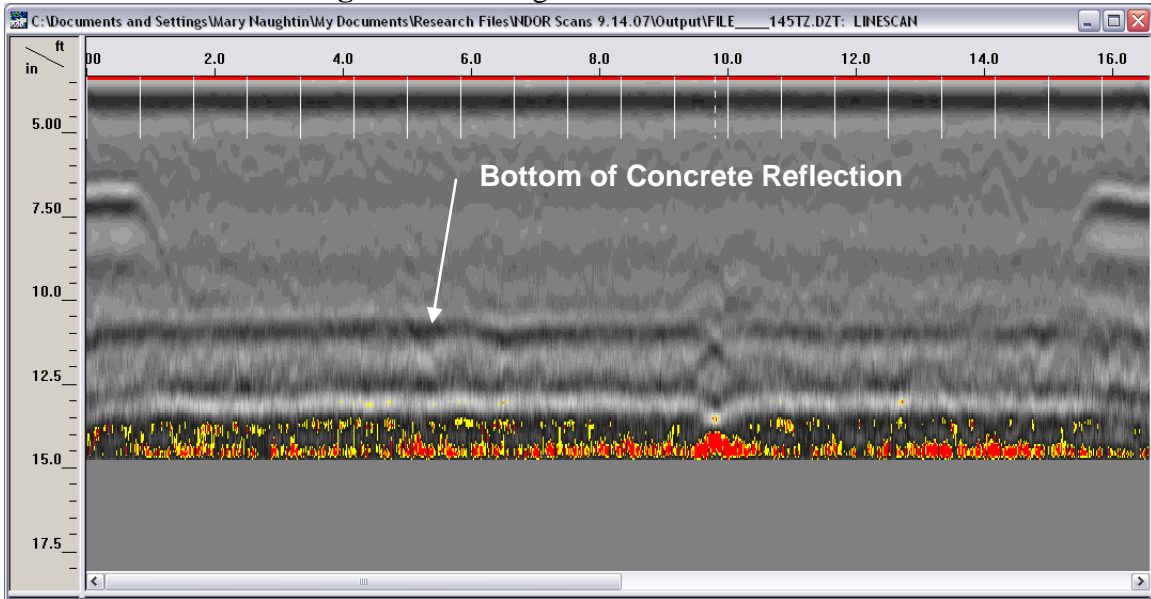


Figure 4.4 Radargram at Station 330 + 80

Another scan was performed on the same day at the last station using a 2 ft x 2ft grid and the SIR-20 GPR system. A paper grid was setup as shown in figure 4.5 and several scanned at 4 in. spacing. The bottom of the concrete was not detected due to a malfunction of the equipment at that time.



Figure 4.5 Grid setup at station 325 + 12

4.2 Field Test #2

The second field test was performed on Friday, September 21, 2007 from 11:00 a.m. – 1:30 p.m. at Highway 34 in Lincoln. The temperature was 85°F and the test was attended by NDOR staff members as well as UNL faculty members and graduate students. In this test, two grid scans were performed at two different locations where two 2 in. diameter metal rings (similar to the one used in lab test #1) were put underneath 10 in. thick concrete pavement.

4.2.1 Scan #1

A 2 ft x 2ft grid was made as shown in figure 4.6 so that the center of the grid is the marked location of the metal ring. The SIR 20 GPR system was used to scan the grid at 4 in. spacing. Figure 4.7 and 4.8 show snapshots from the radargrams of the x-direction and y-direction scans respectively. These figures demonstrate that the bottom surface of the concrete was clearly detected at 10 in. deep as indicated by the signal reflections marked by the green lines. Also, the metal ring underneath the concrete was detected, but less clearly, at the same

depth as indicated by the hyperbolas enclosed by the red circles. It should be noted that the metal ring was detected at a different location from the marked one as shown in figure 4.9. A concrete core was extracted at the marked location (i.e. grid center), but the ring was not found. Another concrete core was extracted later and the ring was found at the location detected by GPR.



Figure 4.6 Grid used for scan # 1

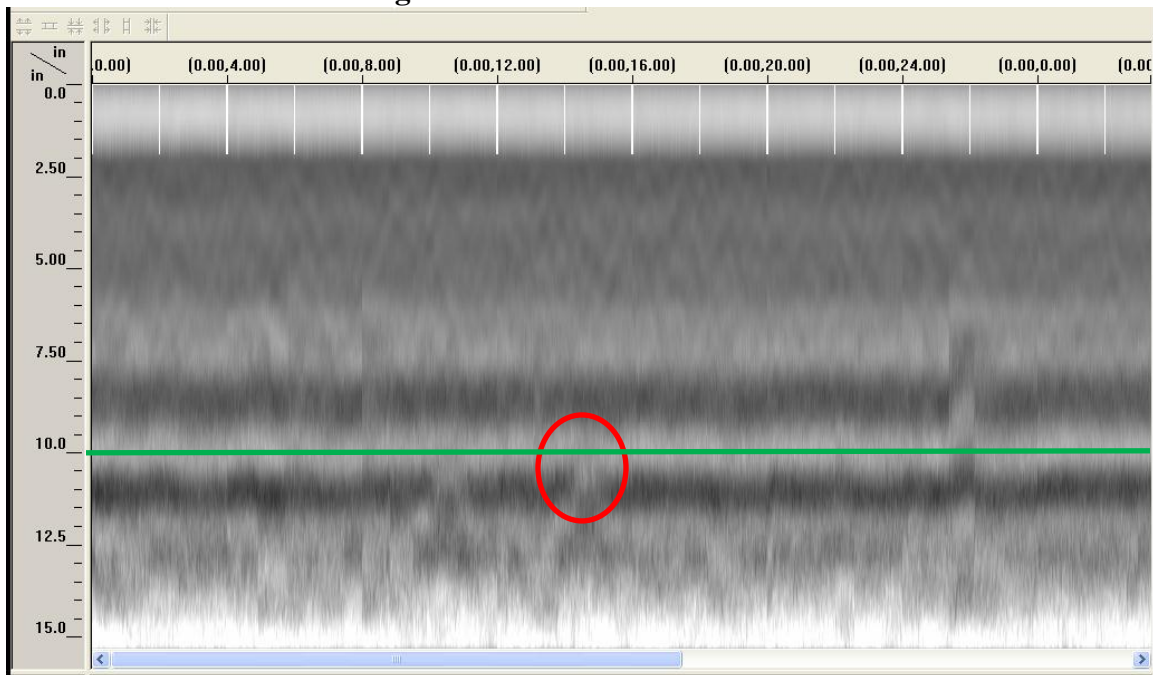


Figure 4.7 Radargram of the x-direction scans (Scan #1)

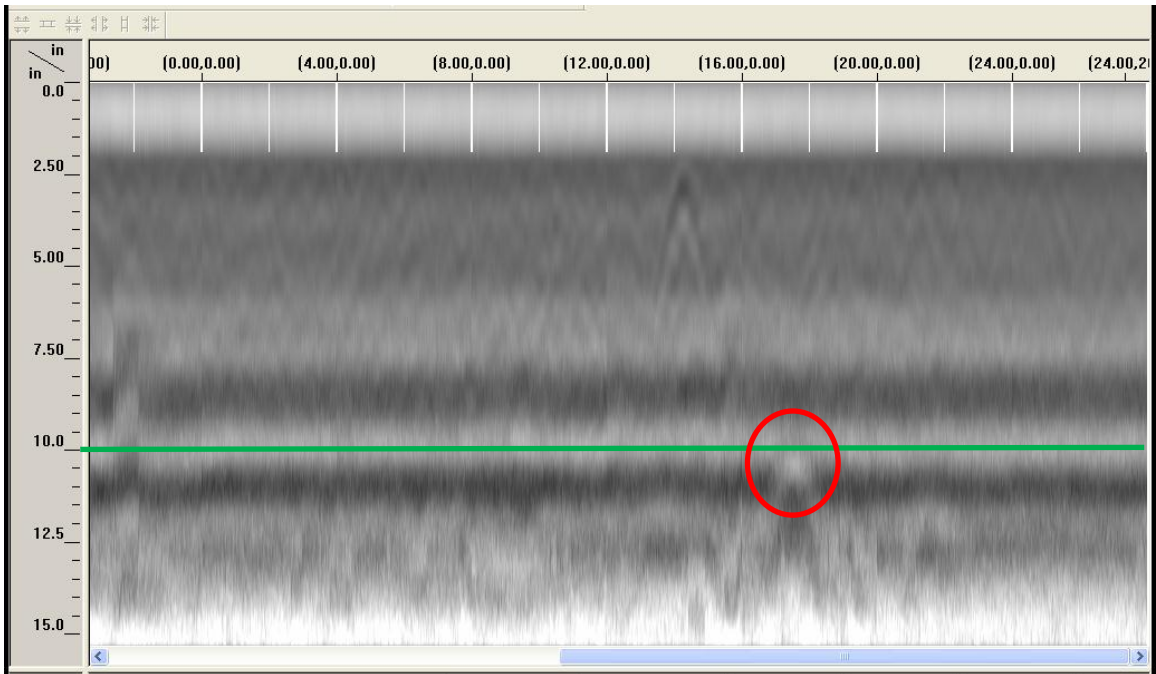


Figure 4.8 Radargram of the y-direction scans (Scan #1)

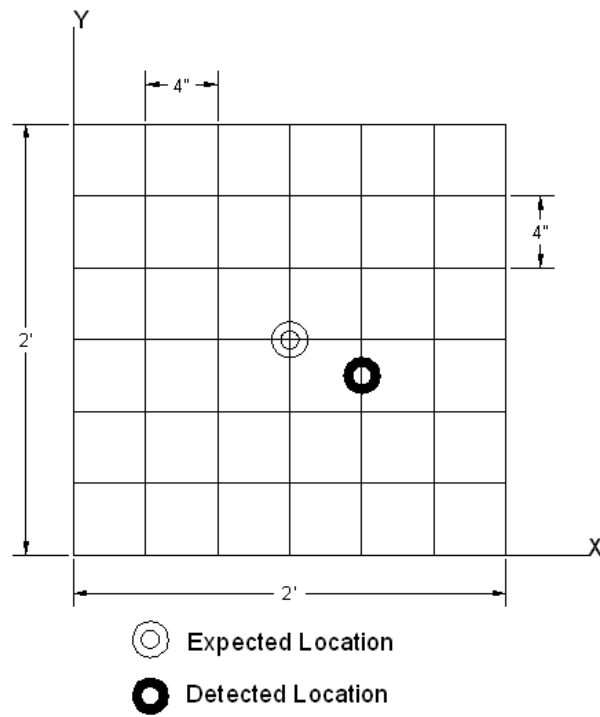


Figure 4.9 Marked and detected locations of the metal ring on the grid of scan #1

4.2.2 Scan #2

A 2 ft x 2ft grid was made as shown in figure 4.10 so that the center of the grid is the marked location of the metal ring. The SIR 20 GPR system was used to scan the grid at 2 in. spacing to determine the location of the ring more accurately. Figures 4.11 and 4.12 show snapshots from the radargrams of the x-direction and y-direction scans respectively. These figures demonstrate that the bottom surface of the concrete was clearly detected at 10 in. deep as indicated by the signal reflections marked by the green lines. Also, the metal ring underneath the concrete was detected, but less clearly, at the same depth as indicated by the hyperbolas enclosed by the red circles. The GPR found what was thought to be the metal ring, but the findings were inconclusive. NDOR verified the location using a metal detector, cored that location, and found the metal ring at a different location from the marked one as shown in figure 4.13.

Based on the results of the two scans performed in the field test # 2, it was concluded that the grid scan using SIR-20 GPR system is more accurate for measuring concrete pavement thickness when metal objects are placed between the concrete and the base layer. It is recommended that metal objects with larger surface than the 2 in. diameter rings be used to clearly and accurately detected the bottom surface of the concrete. These recommendations have been considered in field test # 3. It should be noted that in case of accidental movement of the metal object during concrete pouring and/or vibration, several scans need to be taken to identify the object location, which negatively affect the efficiency the technique.

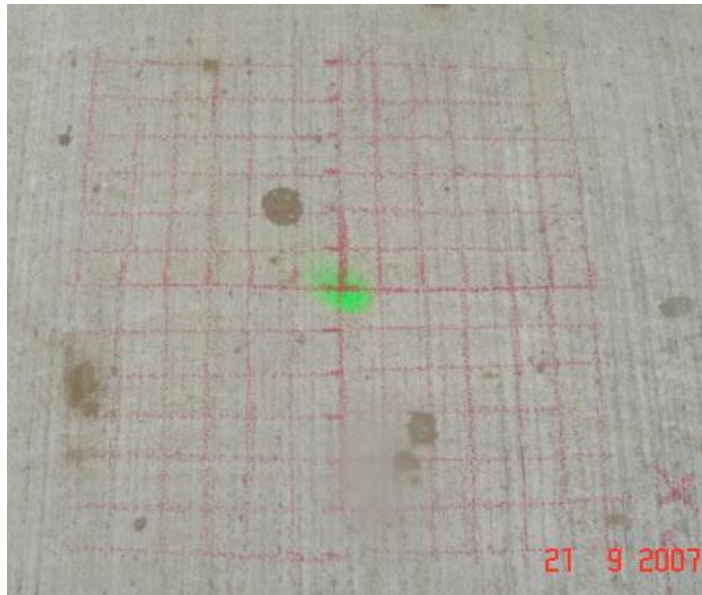


Figure 4.10 Grid used for scan # 2

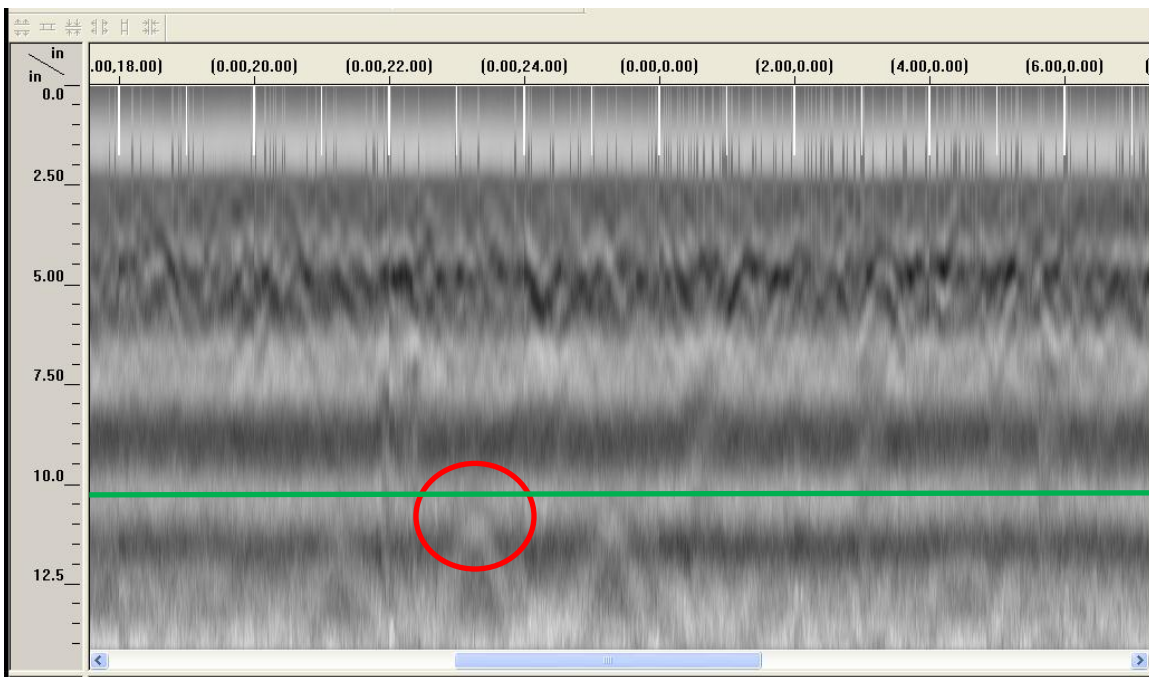


Figure 4.11 Radargram of the x-direction scans (Scan #2)

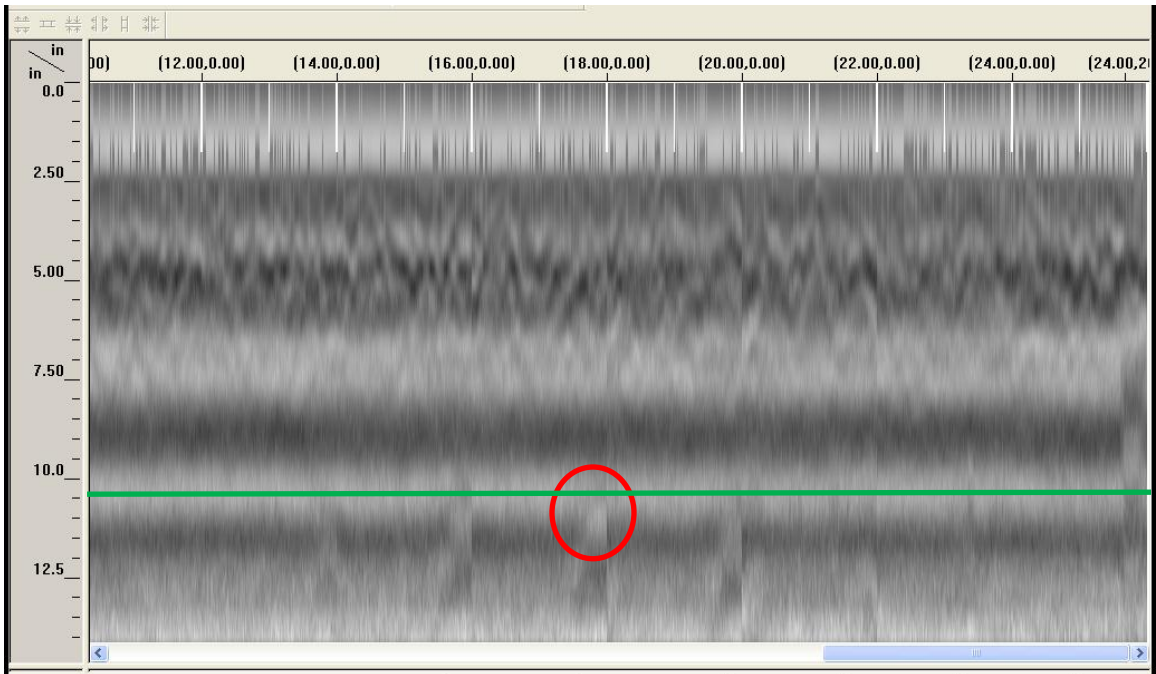


Figure 4.12 Radargram of the y-direction scans (Scan #2)

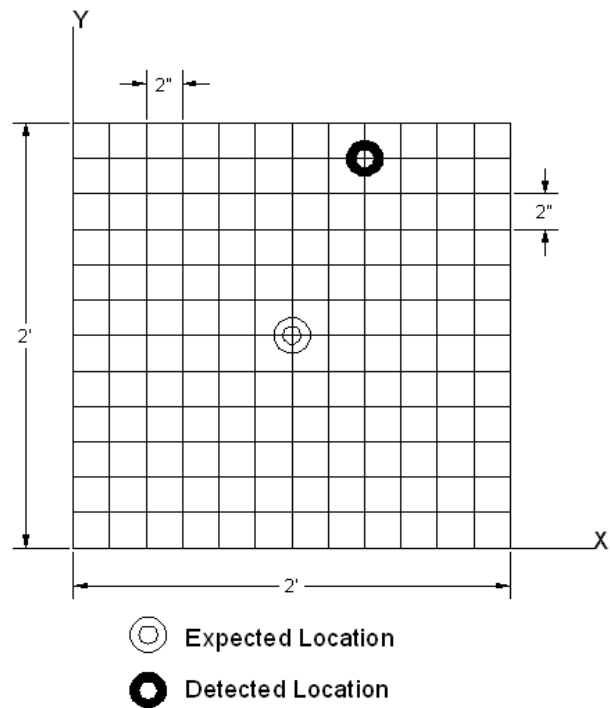


Figure 4.13 Marked and detected locations of the metal ring on the grid of scan #2

4.3 Field Test # 3

The third field test was performed on Monday, June 30, 2008 between 8:30 am – 10:00 am at the Fremont Bypass on Highway 30. Exact location is marked by a red rectangle on the map shown in figure 4.14. The temperature was 80°F and the test was attended by NDOR staff and UNL faculty and graduate students. Eight GPR grid scans were performed at the 8 stations listed in Table 4.2 where zinc steel clad plates were placed on the compacted base before paving. Figure 4.15 show the plate that is 11.8 in. diameter and ¼ in. thick. These plates were used to evaluate the reliability of a relatively new non-destructive evaluation (NDE) technique, known by MIT (Magnetic Imaging Technology) Scan-T2 system. This system for measuring the thickness of concrete pavement is commercially available and was provided to NDOR by the Technology Implementation Group (TIG) as a loan, which is supported by the Federal Highway Administration. After curing, the location of each plate was marked on the concrete surface based on MIT-Scan-T2 readings, which proved to be very accurate in all locations.

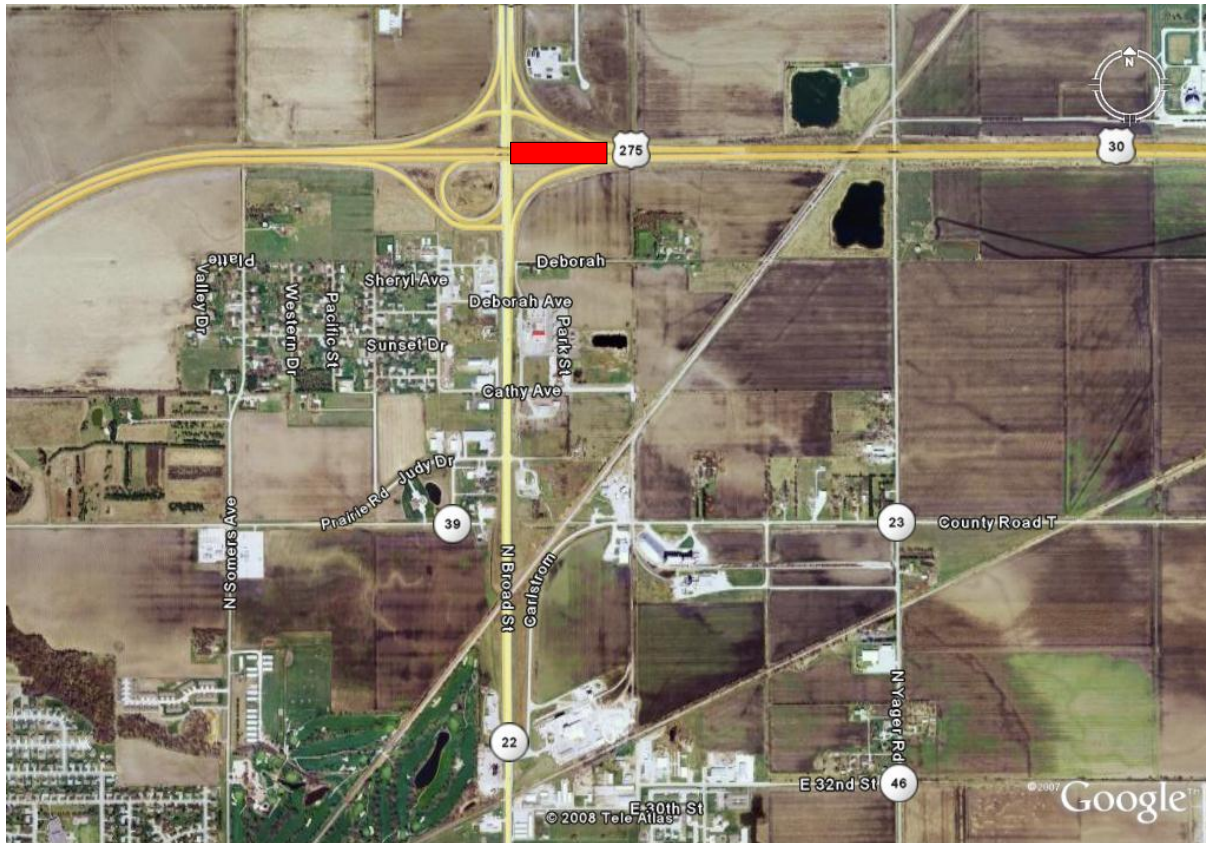


Figure 4.14 Location of the GPR scanned concrete pavement on Highway 30 in Fremont, NE

Table 4.2 Locations of plates scanned in field test #3

Plate	Station
1	49+07
2	48+22
3	47+95
4	47+75
5	45+00
6	44+62
7	44+00
8	44+20



Figure 4.15 Steel plate placed underneath the concrete pavement

At each marked location, a 2 ft x 2 ft grid was placed and GPR grid scans were performed at 4 in. spacing as shown in figure 4.16. It should be noted that performing the eight grid scans took about 40 minutes (i.e. 5 minutes per scan). In all the locations, the steel plate placed at the interface between the bottom surface of concrete and the base layer was clearly detected as indicated by the strong signal reflections at the plate location as shown in figure 4.17. Radargrams of all the 8 stations scanned in this field test are shown in Appendix B.



Figure 4.16 Grid scan at the marked location of the steel plate

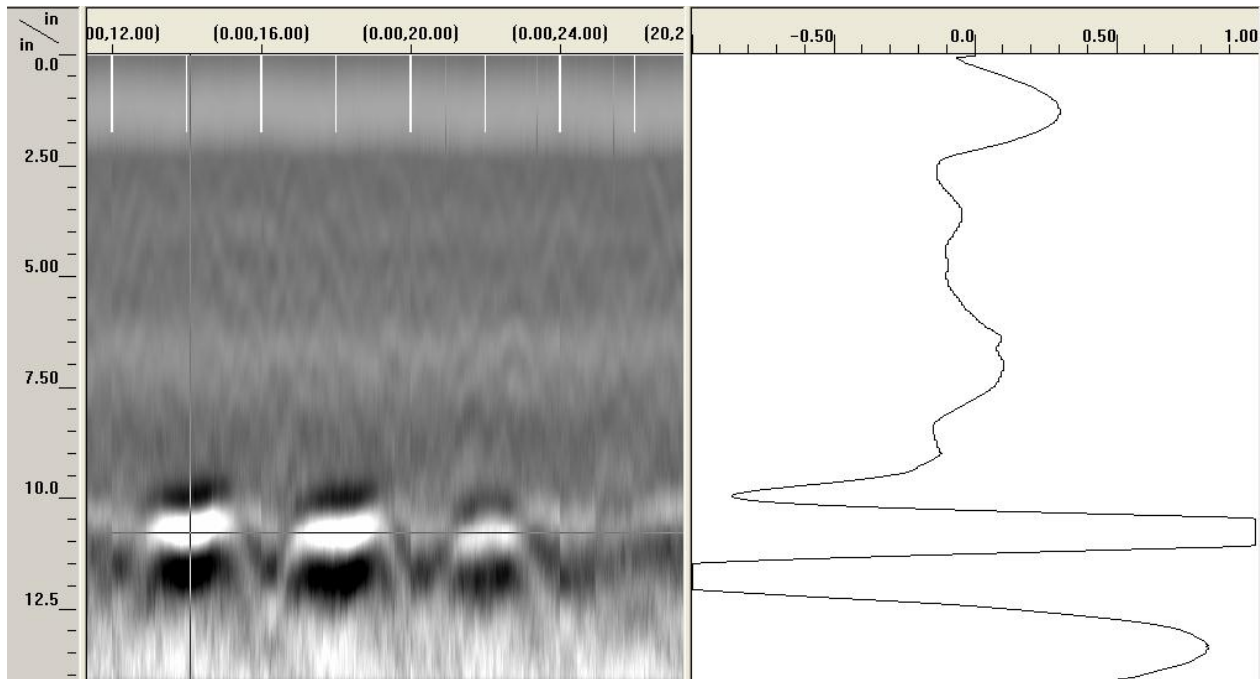


Figure 4.17 Radargram of the GPR grid scan at one station in field test # 3

NDOR took cores at plate locations where the MIT-Scan T2 readings specified it on July 2, 2008. Actual concrete thickness of the two cores located at plates # 2 and # 7 were used to calibrate the GPR scans (i.e calibration cores). The initial dielectric constant used in all the scans

was assumed to be 6.25 (i.e. equipment default value for fairly dry concrete). The actual dielectric constant of the concrete was calculated using the known thickness of calibration cores. This value was found to be 7.23, which is higher than the initial value due to the early age of the concrete and its higher moisture content. The difference between the initial and actual dielectric constants of the concrete resulted in a correction factor for GPR thickness measurements of 0.93. This correction factor was used to adjust GPR thickness measurements of the remaining six plates. Table 4.3 lists the GPR initial thickness measurements, corrected thickness measurements, and actual thickness measurement using 9-point readings of extracted cores (i.e. verification cores). The average of absolute differences in thickness measurement were found to be approximately ¼ in. (2.9 %) when all readings were considered. The average of absolute differences in thickness measurement were found to be approximately 1/8 in. (1.4 %) when reading # 4 is eliminated. This is because the error in reading # 4 was found to be unreasonably high. Same conclusion was confirmed for the same reading using MIT Scan-T2 system.

Table 4.3 Results of field test #3

Plate	Station	GPR-measured thickness (in)	Corrected GPR-measured thickness (in)	Actual Thickness (in)	Difference between Actual and GPR-measured thickness(in)	Difference between Actual and GPR-measured thickness(%)
1	49+07	10.7	9.96	9.70	0.26	2.7%
2	48+22 *	11.3	10.52	10.49	0.03	0.3%
3	47+95	11.6	10.80	10.67	0.13	1.2%
4	47+75	10.2	9.50	8.64	0.86	9.9%
5	45+00	9.0	8.38	8.44	0.06	0.7%
6	44+62	9.3	8.66	8.75	0.09	1.0%
7	44+00 *	8.9	8.29	8.31	0.02	0.3%
8	44+20	10.1	9.40	9.26	0.14	1.5%
Correction Factor		0.93	Average All		2/8	2.9%
* Calibration Station			Average without #4		1/8	1.4%

4.4 Field Test # 4

The fourth field test was performed on Hwy 2 in Lincoln, NE (location is marked by a red rectangle on the map shown in figure 4.18). The test was performed over two days, Thursday, June 18, 2009 and Friday, June 26, 2009, due to some technical problems with the GPR equipment on the first day. The two tests were attended by NDOR staff and UNL faculty and graduate students. Table 4.4 lists the location of 24 zinc steel clad disks placed on the compacted base before paving to be used as reflectors for thickness measurement using GPR and MIT techniques. Only the shaded stations in table 4.4 were scanned using GPR. The first four scans (test a) were performed on June 18, 2009, while the seven remaining scans (test b) were performed on June 26, 2009. Figure 4.19 shows pictures of placing and anchoring one of the disks on the road before paving by NDOR personnel.



Figure 4.18 Location of the GPR scanned concrete pavement on Hwy 2, Lincoln, NE

Table 4.4 Locations of the 24 disks used in Hwy 2 project

Date Performed	Plate	Stations	Reflector Disk Location- From Edge of the Slab Left- (feet)
05-29-09	1	33+17	8
	2	34+17	8
	3	35+17	9
	4	36+17	9.5
	5	37+17	6.5
	6	38+17	8
	7	39+17	9.5
	8	40+17	7
	9	41+17	9
	10	42+17	3
06-05-09	11	50+09	6
	12	51+09	6
	13	52+09	6
	14	53+09	6
	15	54+09	6
	16	55+09	6
	17	56+17	6
	18	57+17	6
	19	58+17	6
	20	59+17	6
	21	60+22	6
	22	61+22	6
	23	62+22	6
	24	63+22	6



Figure 4.19 Placing reflector disks before paving Hwy 2.

At each marked location, a 2 ft x 2 ft grid is placed and GPR grid scans were performed at 4" spacing as shown in figure 4.20. In all the locations, the steel plate placed at the interface between the bottom surface of concrete and the base layer was clearly detected as indicated by the strong signal reflections at the plate location as shown in figure 4.21.



Figure 4.20 Grid scan at the marked location of the steel disk

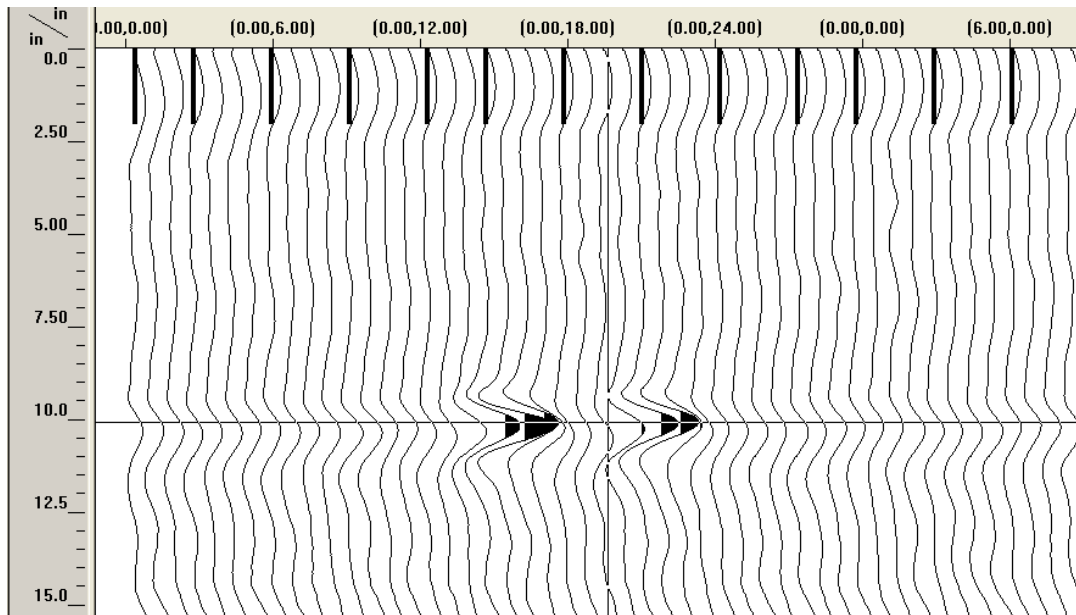


Figure 4.21 Radargram (wiggle mode) of the GPR grid scan at plate # 15

NDOR took cores at all reflector disk locations as specified by the MIT-scan readings. Actual concrete thickness of the two cores located at plates # 3 and # 15 were used to calibrate the GPR scans (i.e calibration cores). The initial dielectric constant used in all the scans was assumed to be 6.25 (i.e. Equipment default value for fairly dry concrete). The actual dielectric constant of the concrete was calculated using the known thickness of calibration cores and was found to be 6.64 and 6.93 for the two tests, which is higher than the initial value due to the early age of the concrete and its higher moisture content. The difference between the initial and actual dielectric constants of the concrete resulted in correction factors for GPR thickness measurements of 0.97 and 0.95 respectively. These correction factors were used to adjust GPR thickness measurements at the remaining locations. Tables 4.5 and 4.6 list the GPR initial measurement, corrected measurements, and the actual thickness measured from extracted cores for the two tests. The average of absolute differences in thickness measurement were found to be approximately 0.11 in. and 0.03 in., which corresponds to 1.2% and 0.4 % for tests a and b, respectively.

Table 4.5 Results of field test #4a

Plate	Station	GPR-measured thickness (in)	Corrected GPR-measured thickness (in)	Actual Thickness (in)	Difference between Actual and GPR-measured thickness(in)	Difference between Actual and GPR-measured thickness(%)
1	33+17	9 3/4	9.44	9.37	0.07	0.7%
3	35+17 *	9 1/2	9.20	9.20	0.00	0.0%
5	37+17	9 3/8	9.08	9.22	0.14	1.5%
4	36+17	9 1/4	8.96	9.18	0.23	2.5%
Average		9 1/2		9.24	0.11	1.2%
Correction Factor		0.97				

Table 4.6 Results of field test #4b

Plate	Station	GPR-measured thickness (in)	Corrected GPR-measured thickness (in)	Actual Thickness (in)	Difference between Actual and GPR-measured thickness(in)	Difference between Actual and GPR-measured thickness(%)
11	50+09	9 3/4	9.26	9.33	0.07	0.70%
13	52+09	9 7/8	9.38	9.31	0.08	0.81%
15	54+09 *	10	9.50	9.50	0.00	0.00%
17	56+17	10	9.50	9.50	0.00	0.00%
19	58+17	10 1/8	9.62	9.61	0.01	0.13%
21	60+22	10	9.50	9.46	0.04	0.41%
23	62+22	9 3/4	9.26	9.22	0.04	0.44%
Average		10	9.43	9.42	0.03	0.36%
Correction Factor		0.95				
* Calibration Station						

4.5 Field Test # 5

The fifth field test was performed at the I-80 west of 56th street in Lincoln, NE (location is marked by a red rectangle on the map shown in figure 4.22). The test was performed on Friday, August 28, 2009 and was attended by NDOR staff and UNL faculty and graduate students. Table 4.7 lists the location of 22 zinc steel clad disks placed on the compacted base before paving to be used as reflectors for thickness measurement using GPR and MIT techniques. Only the shaded stations in table 4.7 were scanned using GPR. Figure 4.23 shows pictures of placing and anchoring one of the disks on the road before paving by NDOR personnel.



Figure 4.22 Location of the GPR scanned concrete pavement on I-80, Lincoln, NE

Table 4.7 Locations of the 22 disks used in I-80 project

Date Performed	Plate	Stations	Reflector Disk Location-Westbound Feet Lt
07-23-09	1	927+00	10
	2	923+00	8
	3	925+03	8
	4	924+03	8
	5	924+03	8
	6	923+05	8
	7	922+02	8
	8	921+00	8
	9	920+00	8
	10	919+00	8
	11	918+00	8
07-24-09	12	917+00	8
	13	916+00	8
	14	915+00	8
	15	914+00	8
	16	913+00	8
	17	912+00	8
	18	911+00	8
	19	910+00	8
	20	910+03	8
	21	909+00	8
	22	908+00	8



Figure 4.23 Placing reflector disk before paving I-80

At each marked location, a 2 ft x 2 ft grid is placed and GPR grid scans were performed at 4” spacing as shown in figure 4.24. In all the locations, the steel plate placed at the interface between the bottom surface of concrete and the base layer was clearly detected as indicated by the strong signal reflections at the plate location as shown in figure 4.25.

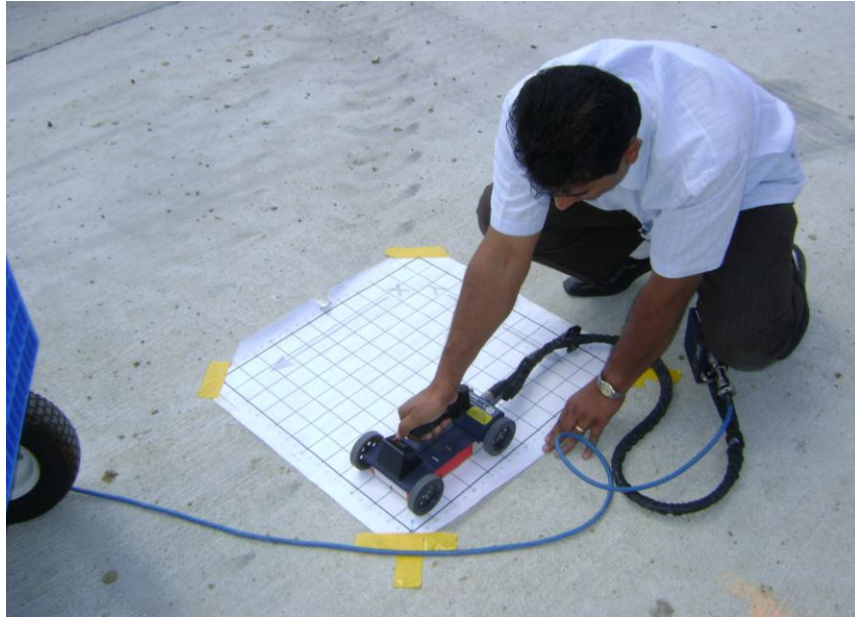


Figure 4.24 Grid scan at the marked location of the steel disk

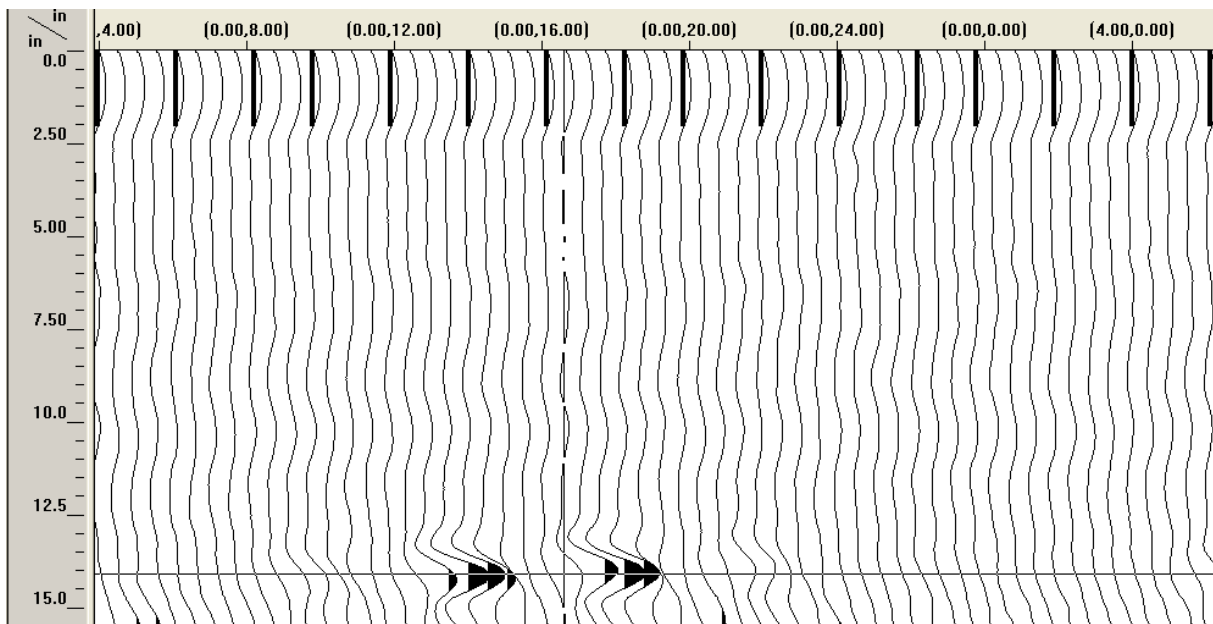


Figure 4.25 Radargram (wiggles mode) of the GPR grid scan at plate # 14

NDOR took cores at all reflector disk locations as specified by MIT-scan readings. Actual concrete thickness of the two cores located at plate # 12 was used to calibrate the GPR scans (i.e calibration core). The initial dielectric constant used in all the scans was assumed to be 6.25 (i.e. Equipment default value for fairly dry concrete). The actual dielectric constant of the concrete was calculated using the known thickness of calibration cores and was found to be 7.07, which is higher than the initial value due to the early age of the concrete and its higher moisture content. The difference between the initial and actual dielectric constants of the concrete resulted in a correction factor for GPR thickness measurements of 0.94. This correction factor was used to adjust GPR thickness measurements at the remaining locations. Table 4.8 lists the GPR initial measurement, corrected measurements, and the actual thickness measured from extracted cores. The average of absolute difference in thickness measurement was found to be approximately 0.1 in., which corresponds to 0.75%

Table 4.8 Results of field test #5

Plate	Station	GPR-measured thickness (in)	Corrected GPR-measured thickness (in)	Actual Thickness (in)	Difference between Actual and GPR-measured thickness(in)	Difference between Actual and GPR-measured thickness(%)
2	9+26	13 1/2	12.68	12.94	0.26	2.03%
4	9+24	13 3/4	12.91	12.89	0.02	0.18%
6	9+22	13 5/8	12.80	12.92	0.12	0.97%
8	9+20	13 7/8	13.03	12.96	0.07	0.54%
10	9+18	13 5/8	12.80	12.99	0.19	1.50%
12	9+16 *	13 7/8	13.03	13.03	0.00	0.00%
14	9+14	14	13.15	13.24	0.09	0.70%
16	9+12	13 5/8	12.80	12.89	0.09	0.74%
18	9+10	14	13.15	13.07	0.08	0.59%
20	9+8	13 7/8	13.03	12.99	0.04	0.31%
Average		13 7/9	12.94	12.99	0.10	0.75%

Correction Factor 0.94

*** Calibration Station**

Chapter 5 Benefit-Cost Analysis

Table 5.1 presents a comparison between the proposed GPR pavement quality assurance technique and the traditional coring technique in terms of cost (initial cost and operating cost) and benefits (accuracy, time and destructiveness). This comparison is based on 1 mile assessments using 8 cores for the traditional method and 8 scans + 2 calibration cores for GPR method. The operating cost was calculated assuming an hourly labor rate of \$50, cost of metal plate of \$8.75, and cost of core drilling and filling material as \$2.50. Time was calculated assuming 10 minutes for core extraction, 5 minutes for core thickness measurement using 9 point reading, 5 minutes for one GPR scan, and 10 minutes for GPR scan analysis. These estimates were based on the investigators' experience in this project and information provided by NDOR personnel.

Table 5.1 Benefit-Cost Comparison Between GPR and Coring

Criteria	GPR (8 scans + 2 cores)	Coring (8 cores)
Destructiveness	Nondestructive	Destructive
Accuracy	98.50%	100%
Time	$8 \times (5 + 10) + 2 \times (10 + 5) = 2.5$ hrs	$8 \times (10 + 5) = 2$ hrs
Initial Cost	\$35,000	0
Operating Cost	\$200	\$120

Based on this table, it can be concluded that the major advantage of using GPR in concrete pavement thickness measurement is the significant reduction in the number of drilled cores, which is a destructive technique that affect the pavement durability, while providing a comparable accuracy. The proposed methodology provided an accuracy as high as 98.5% (1/8 of

inch), which is better than the values presented in the literature. Although GPR equipment has higher initial and operating cost than core drilling, the minimization of core drilling might result in lower pavement maintenance cost in the long term. It should be noted that, as with any new technique, attention must be paid to proper training for GPR to provide reliable and consistent results in a cost-effective fashion. Also, the lack of specifications is an important limitation and needs to be addressed.

Chapter 6 Summary and Conclusions

In this project, the feasibility of the use of GPR as a non-destructive evaluation technique for measuring the thickness of concrete pavement was investigated. Currently, NDOR performs thickness measurement of concrete pavement according to ASTM C174. Although this method provides an accurate thickness measurement, it is destructive, labor intensive, and time consuming. Moreover, concrete cores are usually extracted every 750 ft, which provides inadequate information about the thickness profile of pavement sections. The GPR technique was proposed because of its advantages over drilled cores, such as being non-destructive, user friendly, efficient, and cost-effective when applied to long pavement sections. However, the literature of using GPR for measuring the thickness of concrete pavement does not provide sufficient evidence regarding accuracy and consistency. Therefore, the objective of this project was to investigate GPR's accuracy relative to drilled cores in measuring thickness of concrete pavement for quality assurance purposes. The GPR systems GSSI SIR20 and GSSI SIR3000 with a high resolution 1.6 MHz ground coupled antenna were used. Three laboratory tests and three field tests were performed within this project. Different metal objects were used underneath the concrete to improve GPR signal reflectivity at the bottom surface of the concrete pavement. Also, GPR scans were performed at different concrete ages to estimate the variation in the dielectric constant of the concrete.

Based on the results of the lab and field tests, the following conclusions were made:

1. GPR is an efficient technique for measuring the thickness of concrete pavement. Grid scans can be performed in as short as 5 minutes per location, while data analysis can be as low as 10 minutes per scan.

2. GPR signal reflections at the interface between the bottom of the concrete layer and the base layer are neither clear nor reliable due to the proximity of the dielectric constant of the concrete and that of the base layer.
3. GPR signal reflections at the interface between the bottom of the concrete layer and the base layer are clear and reliable when metal objects are placed on the top of the base layer before paving. Although GPR can accurately locate these objects, it is recommended for rapid evaluation that the objects be anchored properly so they do not shift while pouring and/or vibrating the concrete.
4. The surface area of the metal object used is more important than its thickness for being easily and clearly detected by GPR. Flat objects, such as plates, with rectangularity ratio close to 1, are more efficient than narrow and long objects, such as rods or strips.
5. The dielectric of the concrete is highly dependent on the concrete age, which significantly affects the measured thickness. The lab test results indicated that using a constant value of the concrete dielectric results in a significant reduction in the measured thickness of 0.01 in. per day as the concrete gets older. That is why calibration cores are needed.
6. Calibration cores are necessary for correcting the assumed value of dielectric constant of concrete. Based on the field test results, one or two drilled cores are satisfactory for calibrating ten readings.

The average difference in concrete thickness measurements using GPR (with calibration cores) and drilled cores is found to be 1/8 in. for 10 - 13 in. thick pavement. This represents an average measurement accuracy of 98.5%, which is relatively high. It should be noted that the

accuracy of GPR measurements is highly dependent on the calibration process, which requires the extraction of a limited number of cores

Chapter 7 Implementation Plan

One of the objectives of this research was to evaluate the feasibility of using GPR for measuring pavement thickness. While this research was taking place, NDOR's In-House Research was also evaluating other products for measuring pavement depth. As a result of these evaluations, some of the conclusions drawn from this study have put into question how effective the GPR compares with other products for measuring pavement depth. NDOR has found other equipment requires no calibration, saves time with less data input, is easier to use and costs less. NDOR is still evaluating other products that are in the market today. Therefore, the Department will not implement the GPR equipment at this time.

Wally Heyen

NDOR Portland Cement Concrete Engineer

References

- Al-Qadi, I. L., and S. Lahour. 2004. "Ground Penetrating Radar: State of the Practice for Pavement Assessment." *Journal of Materials Evaluation*, 42, no. 7: 759-763.
- ASTM. 2006a. "Standard Test Method for Determining the Thickness of Bound Pavement Layers Using Short-Pulse Radar." Standard D4748-06 ASTM International, West Conshohocken, PA.
- ASTM. 2006b. "Standard Test Method for Measuring Thickness of Concrete Elements Using Drilled Concrete Cores." Standard C174/C174M-06, ASTM International, West Conshohocken, PA.
- Federal Highway Administration. 2004. *Priority, Market-Ready Technologies and Innovations: Ground-Penetrating Radar*. Washington D.C., US Department of Transportation.
- Kurtz, James, Bouzid Choubane, Emmanuel Fernando. 2001. *Improved Roadway Subsurface Thickness Measurement and Anomaly Identification with Ground Penetrating Radar*. Tallahassee, FL, Florida Department of Transportation.
- Loulizi, A., I. L. Al-Qadi, and S. Lahouar. 2003. "Optimization of Ground-Penetrating Radar Data to Predict Layer Thickness in Flexible Pavements." *ASCE Journal of Transportation Engineering*, 129, 1: 93-99.
- Maierhofer, C. 2003. "Nondestructive Evaluation of Concrete Infrastructure with Ground Penetrating Radar." *ASCE Journal of Materials in Civil Engineering*, 15, no. 3: 287-297.
- Maser, K. R. 1996. "Condition Assessment of Transportation Infrastructure Using Ground-Penetrating Radar." *ASCE Journal of Infrastructure Systems*, 2, no. 2: 94-101.
- Olhoeft, Gary, Stanley Smith. 2000. "Automatic Processing and Modeling of GPR Data for Pavement Thickness and Properties." *Proceedings, Eighth International Conference on Ground Penetrating Radar*. Gold Coast, Australia.
- Willett, D. A., K.C. Mahboub, and B. Rister. 2006 "Accuracy of Ground-Penetrating Radar for Pavement-Layer Thickness Analysis." *ASCE Journal of Transportation Engineering*. 132, no. 1: 96-103.

Appendix A

Construction Photos of the Test Driveway

Leveling



Forming



Compacting Subgrade



Embedding Objects



Pouring Concrete



Vibrating and Finishing



Covering of Concrete



Coring

